Investigation of Mechanical Properties of Aluminum: Molecular Dynamics Approach

By

© Sabir Subedi

A Thesis submitted to the School of Graduate Studies
In partial fulfillment of the requirements for the degree of

Master of Engineering

Faculty of Engineering and Applied Science
Department of Mechanical Engineering

Memorial University of Newfoundland
St. John's, Newfoundland and Labrador, Canada

May 2020

St. John's Newfoundland

Abstract

In the present study, the mechanical properties of a single crystal and nanocrystalline aluminum were investigated. The systems were deformed under uniaxial loading at atomistic level. First, the investigation was performed to predict the accuracy of various many-body interatomic potentials available on estimating the mechanical properties of single crystal aluminum. As such, results from the current simulations were compared with available experimental data from references. From the study, it was demonstrated that potentials which were parameterized for the elastic constants at room temperature showed high accuracy with the experimental data. Out of fourteen potentials tested in the current research, the Mishin et al. EAM potential predicted the most accurate mechanical properties for single crystal aluminum. Next, this potential was used to simulate uniaxial deformation for nanocrystalline aluminum. Results showed good agreement with available experimental data for nanocrystalline aluminum. The effects of various grain sizes, strain rates, and temperatures were investigated. It was observed that the stacking faults, sliding of the grain boundaries, and nucleation of atoms near grain boundaries during deformation hardened the nanocrystalline material as the grain diameter increased, which is reverse Hall-Petch relationship.

Acknowledgements

I would like to acknowledge some special persons who always encouraged and motivated me to achieve the best in my life. First, I am very grateful to Dr. Sam Nakhla for giving me the opportunity. You made my two years in Canada much easier. You were always there when I needed you the most, as a supervisor and a family member. You inspired and pushed me to extend my boundaries of learning, which helped me to successfully complete this degree. You always taught me to be a team player. Once again, thank you for your unforgettable support and caring.

To my parents, Prashuram and Manju Subedi, thank you for teaching me the value of the education throughout my life and encouraging me in every steps. Thank you for blessings and unconditional love for me. To my brother and sister in law, Samir and Bhumika Subedi, thank you for your love and guidance. You always force me to dream big. To my backbone, my sister and brother in law, Sony and Kiran Ghimire, thank you for all your support. To my girlfriend, Shova Dahal, thank for standing beside me through the whole journey of my degree. Your support and encouragement pushed me to be a better person.

To my Team, Ahmed Elruby, Liam Morrissey, Stephen Handrigan, and Douglas Pratt, thank you for your continuous support and all the helpful suggestions for my research. I am blessed to have shared the same office room with you all.

Finally, I would like to thank Bombardier Inc., and Research and Development Corporation (RDC) for the financial support.

Table of Contents

List of Tables

List of Figures

List of Abbreviations and Symbols

MD	Molecular Dynamics
FCC	Face Centered cubic
BCC	Body Centered Cubic
HCP	Hexagonal Close Packed
EAM	Embedded Atom Model
MEAM	Modified Embedded Atom Model
ReaxFF	Reactive Force Field
EMT	Effective Medium Theory
nm	Nanometer
ps	Picosecond
s^{-1}	per second
Å	Angstrom
LAMMPS	Large-scale Molecular Massively Parallel Simulator

1. Chapter 1: Introduction

1.1. Background

With the increasing computational power, Molecular Dynamics (MD) simulations, an atomistic approach, are gaining the interest of researchers from different disciplines such as chemistry, material science, bio-medical, and nano-technology. In recent years, many studies on estimating the mechanical properties of metals at the atomistic level, either single crystal or nanocrystalline structure, were performed. There is some literature for the uniaxial tension test of a single crystal metal in MD simulation. Komanduri et al. [1] have investigated the mechanical behavior of various single-crystal cubic metals with crystal orientation <1 0 0>, such as Face Centered Cubic (FCC) (Aluminum, Copper, and Nickel) and Body Centered Cubic (BCC) (Iron, Chromium, and Tungsten) using MD simulation of uniaxial tension test. The simulations were performed at room temperature at a constant strain rate (5 Å/ps) using Morse potential for the various metals. Results showed the strain to fracture behavior of the FCC and BCC metals. Furthermore, the authors concluded that the parameterization of the potentials was needed for the simulations, as the Morse potentials did not account the deformation behavior of the BCC metals as accurately as the FCC metals. However, there were no comparisons of different types of available potentials. Similarly, Yang et al. [2] estimated Young's modulus and Poisson's ratio for a single crystal copper nanorod under uniaxial tensile loading using MD simulation. The authors investigated the effect of crystallographic orientations and cross-section sizes of the simulation box on estimating mechanical properties using Embedded Atom Method (EAM) potentials at 0 K. However, the accuracy of the potential used was not verified. Furthermore, there was no comparison of the results obtained with available test data.

In MD, an interatomic potential is needed to calculate the interatomic forces and acceleration between the interacting atoms and molecules. Hence, the importance of the parameterization of the potential based on the applications is required for the MD simulation. Very few literatures [3-5] are available, which have tested different potentials for various metals such as iron, molybdenum, silicon, titanium, zirconium, and magnesium. Morrissey et al. [3] investigated various many-body potentials for their ability to predict the mechanical properties of single crystal iron. The authors simulated a uniaxial tension test at room temperature at an atomistic-level using various potentials, i.e. EAM, MEAM, ReaxFF, and Tersoff. Further, results were compared with experimental data to show the accuracy of the potentials used. Tersoff and ReaxFF were the most accurate indicating the importance of bonding during the atomistic simulations. Similarly, Etesami et al. [4] calculated the elastic constants for the various interatomic potentials for titanium, zirconium, and magnesium. Results obtained were compared with available experimental data. The authors have discussed the transferability of the potential and concluded the most accurate interatomic potentials for the high-temperature materials. In addition, Lysogorskiy et al. [5] quantified the accuracy and transferability of the interatomic potential for molybdenum and silicon by comparing the results from the simulation to the available experimental data for the material properties, such as cohesive energy, atomic volume, elastic coefficients, vibrational properties, thermodynamics properties, surface energies and vacancy formation energies. It has been demonstrated from these works that the interatomic potential has strengths and weaknesses based on the application. Hence, these works concluded that the assessment for the parameters of the interatomic potential is necessary to be appropriately studied before any simulation performed.

From the previously cited literature, it is clear that the interatomic potential is parameterized based on the application for various metals. However, there is insufficient literature available for the testing of different many-body potentials for FCC metals. Hence, an assessment of the various many-body interatomic potentials was performed utilizing MD simulations of uniaxial loading at room temperature for a single crystal aluminum with crystal orientation <1 0 0>. Elastic modulus and Poisson's ratio were compared with available experimental data to quantify the accuracy of the interatomic potentials for FCC aluminum.

While single-crystal metals were used to verify the accuracy of the interatomic potentials, they are not representative of the microstructure of typical metals. Typical engineering metals possess a polycrystalline structure. As such, a nanocrystalline sample was constructed and simulated in MD to replicate the macroscale testing. A nanocrystalline structure is a polycrystalline material where the grain size is in the nanometer (nm) scale. In recent years, researchers are highly interested in investigating the mechanical properties of nanocrystalline metals due to their various applications such as high-efficiency gas turbines, aerospace, and automotive components, which was discussed by Suryanarayana [6]. As such, there are some significant literature on estimating the mechanical properties of nanocrystalline metals in MD simulations which compared to experimental data. One example is the work by Schiotz et al. [7]. The authors investigated the mechanical deformation of nanocrystalline copper using MD simulations of uniaxial loading with the Effective Medium Theory (EMT) potential [8]. Effect of grain size, temperature and strain rate on elastic and plastic behavior of nanocrystalline copper were shown. Results demonstrated that the decrease of grain size lead to the increase in the number of grain

boundary atoms, which caused the under-prediction of elastic modulus of a nanocrystalline material as compared with experimental data. As well, the movement of dislocation through the grain and nucleation of the atoms near grain boundary decreases the yield and flow stress. As such, the inverse Hall-Petch relationship, i.e. the increment of grain size lead to the hardening of nanocrystalline copper, was studied. Furthermore, it was shown that the metal becomes softer with increased temperature. Similarly, Galanis et al. [9] also studied the mechanical response of nanocrystalline copper. The deformation was performed in MD simulation using the same many-body EMT potential from Schiotz et al. [7]. Results showed the estimation of elastic modulus, Poisson's ratio, and cohesive energies of the system and compared with available experimental data. Similar to Schiotz's work, they concluded the softening of copper at small grain sizes due to the increase of grain-boundary atoms. In addition, there is some literature available for nanocrystalline aluminum. Xu et al. [10] performed a uniaxial tensile deformation for nanocrystalline aluminum with various mean grain sizes. A comprehensive classical MD simulation was carried out using the Mishin et al. EAM potential [11] at room temperature. Here, the grain size dependence tensile nano-mechanics were investigated. The results demonstrated the complete Hall-Petch relationship for the nanocrystalline aluminum bulk, identifying distinct regions including the normal, reverse, and extended areas. However, the effect of the strain rate and change in structure were not investigated for nanocrystalline aluminum. Kadau et al. [12] also investigated the mechanical deformation in MD for nanocrystalline aluminum. The MD simulations were performed using an EAM potential using Scalable Parallel Short-range Molecular dynamics (SPaSM). The authors focused more on the preparation of nanocrystalline system than estimating the elastic modulus and Poisson's ratio for various

grain sizes. As such, two different sample preparation methods, Voronoi Construction and Sintered under pressure and temperature, were used to construct a nanocrystalline aluminum structure. The system that was built using Voronoi method has no pores and possesses different mechanical properties than that of the sample prepared using the sintered method. However, the sintered system has a low-density as it contains pores in the system. Results demonstrated the inverse Hall-Petch relationship for grain sizes smaller than 10 nm which was validated with the works of Schiotz et al. [7]. In addition, the fractures along the grain boundaries were obtained for the aluminum sample, which was not the same case for the copper sample. However, the effect of temperature and strain rate on estimating elastic modulus and Poisson's ratio were not accounted in these literatures.

Building from the comprehensive literature review, two cases were investigated in the current work. First, single crystal aluminum was simulated in MD under uniaxial loading using various many-body interatomic potentials at room temperature to investigate the accuracy of various interatomic potentials on estimating the mechanical properties. To validate these potentials, results were compared with available experimental data. Second, the most accurate potential from the initial study was used to simulate a nanocrystalline aluminum with various grain sizes at room temperature undergoing uniaxial tension. Furthermore, the simulation procedure was validated with published experimental results. Results showed good agreement to experimental data for both cases. The purpose of this thesis was to demonstrate the importance of the parameterization of the various many-body potentials in MD simulation based on the different applications for various materials. In addition, the mechanical properties, such as elastic modulus and Poisson's ratio, for single crystal and nanocrystalline aluminum system were presented within the current work.

1.2. Thesis Overview and Purpose

The overall purpose of this Master's thesis was to investigate the accuracy of various many-body interatomic potentials on estimating elastic modulus and Poisson's ratio in MD for single crystal aluminum and calculating the mechanical properties for nanocrystalline aluminum with different grain size using the most accurate potential. For this, a simulation box was deformed under uniaxial tensile loading at room temperature. Several types of potentials available, including EAM, Modified EAM (MEAM), and Reactive Force Field (ReaxFF) were used. As a result, stress-strain curves were obtained from the simulations. Within the linear region (ε = 2%) of the stress-strain curves, the elastic modulus and Poisson's ratio were determined and compared with the experimental data.

This thesis is a manuscript based on four chapters.

Chapter 1 has an overall review of the previous literature related to the present study.

Chapter 2 discusses the prediction of the most accurate many-body interatomic potential on estimating the mechanical properties of single crystal aluminum with crystal orientation <1 0 0>. The brief descriptions of MD simulation and the parameterization of the various many-body potentials are provided in this chapter.

Chapter 3 focuses on the calculation of the mechanical properties of nanocrystalline aluminum with various grain sizes. Here, nanocrystalline aluminum is deformed under uniaxial loading using the most accurate interatomic potential identified within Chapter 2. In addition, the construction method of the nanocrystalline structure is described.

Chapter 4 concludes the investigations and results from this study and provides directions for possible future studies.

1.3. Co-authorship Statement

In the present thesis, the research works were a collaborative effort made by the author of this thesis, Liam S. Morrissey, and Stephen M. Handrigan. The contribution of the co-authors is outlined below.

For Chapter 2, the paper titled *the effect of many-body potential type and parameterization on the accuracy of predicting mechanical properties of aluminum using molecular dynamics*; Liam S. Morrissey and Stephen M. Handrigan contributed. For this paper, all three authors discussed and prepared the research proposal. The author of this thesis performed all simulations, analysis of the results, and manuscript preparation. Liam S. Morrissey and Stephen M. Handrigan assisted with editing and organizing the paper. This paper was accepted in Taylor & Francis' journal *Molecular Simulation.*

For Chapter 3, the paper titled *Mechanical properties of nanocrystalline aluminum: a molecular dynamics investigation,* Liam S. Morrissey and Stephen M. Handrigan contributed. The author of this thesis prepared the research proposal and literature review, performed all simulations, analyzed the results, and prepared the initial manuscript. The co-authors assisted with modifying the manuscript. Stephen M. Handrigan and Liam S. Morrissey are the second and third author respectively. The manuscript is currently undergoing revisions prior to submission.

References

1. Komanduri, R., Chandrasekaran, N., and Raff, L. M. (2001). Molecular dynamics (MD) simulation of uniaxial tension of some single-crystal cubic metals at the nanolevel. *International Journal of Mechanical Sciences*, *43*(10), 2237-2260.
2. Yang, Z., Yang, Q., and Zhang, G. (2017). Poisson's ratio and Young's modulus in single-crystal copper nanorods under uniaxial tensile loading by molecular dynamics. *Physics Letters A*, *381*(4), 280-283.
3. L. S. Morrissey, S. M. Handrigan, S. Subedi, and S. Nakhla, "Atomistic uniaxial tension tests: investigating various many-body potentials for their ability to produce accurate stress-strain curves using molecular dynamics simulations*," Molecular Simulation, pp. 1-8, December 2018.*
4. S. A. Etesami, M. Laradji, and E. Asadi, "Interatomic potentials transferability in predicting temperature dependency of elastic constants for titanium, zirconium, and magnesium," *Modelling and Simulation in Materials Science and Engineering*, *vol. 27, January 2019.*
5. Y. V. Lysogorskiy, T. Hammerschmidt, J. Janssen, J. Neugebauer and R. Drautz, "Transferability of interatomic potentials for molybdenum and silicon" *Modelling and Simulation in Materials Science and Engineering, vol. 27, January 2019.*
6. Suryanarayana, C. (1995). Nanocrystalline materials. *International Materials Reviews, 40(2), 41-64.*
7. Schiøtz, J., Vegge, T., Di Tolla, F. D., and Jacobsen, K. W. (1999). Atomic-scale simulations of the mechanical deformation of nanocrystalline metals. *Physical Review B*, *60*(17), 11971.

8. Jacobsen, K. W., Stoltze, P., and Nørskov, J. K. (1996). A semi-empirical effective medium theory for metals and alloys. *Surface Science*, *366*(2), 394-402.
9. Galanis, N. V., Remediakis, I. N., and Kopidakis, G. (2010). Mechanical response of nanocrystalline Cu from atomistic simulations. *physica status solidi c*, *7*(5), 1372-1375.
10. Xu, W., and Dávila, L. P. (2018). Tensile nanomechanics and the Hall-Petch effect in nanocrystalline aluminium. *Materials Science and Engineering: A*, *710*, 413-418.
11. Mishin, Y., Farkas, D., Mehl, M. J., and Papaconstantopoulos, D. A. (1999). Interatomic potentials for monoatomic metals from experimental data and ab initio calculations. *Physical Review B*, *59*(5), 3393.
12. Kadau, K., Lomdahl, P. S., Holian, B. L., Germann, T. C., Kadau, D., Entel, P., and Westerhoff, F. (2004). Molecular-dynamics study of mechanical deformation in nano-crystalline aluminum. *Metallurgical and materials transactions A*, *35*(9), 2719-2723.

2. Chapter 2: The effect of many-body potential type and parameterization on the accuracy of predicting mechanical properties of aluminum using molecular dynamics

Abstract:

As opposed to traditional laboratory testing, Molecular Dynamics (MD) offers an atomistic scale method to estimate the mechanical properties of metals. However, there is limited literature that shows the effect of interatomic potentials when determining mechanical properties. Hence, the present research was conducted to investigate the accuracy of various interatomic potentials in estimating mechanical properties of aluminum. Several types of potentials, including Embedded Atom Method (EAM), Modified EAM (MEAM) and Reactive Force Field (ReaxFF) were compared with available experimental data for pure aluminum to determine the most accurate interatomic potential. A uniaxial tensile test was performed at room temperature using MD simulations for nanoscale aluminum. Results demonstrated that those potentials parameterized with elastic constants at physically realizable temperatures were consistently more accurate. Overall, the Mishin et al. EAM potential was the most accurate when compared to single crystal experimental values. Regardless of the potential type, error was significantly higher for those potentials that did not consider elastic constants during development. In brief, the application of the interatomic potentials to estimate mechanical properties of a nanoscale aluminum was investigated.

2.1. Introduction

Molecular dynamics (MD), a computational method mostly used in the field of theoretical physics and chemistry, has recently become a well-accepted approach in the area of material and medical science. For example, Schiotz *et al.* [1] have investigated the mechanical deformation of nanocrystalline copper using atomistic scale simulations. In addition, Komanduri *et al.* [2] have studied the mechanical properties of some single crystal cubic metals at the nanoscale. In the study, a nanoscale uniaxial tensile test was simulated for Face Centered Cubic (FCC) (Aluminum, Copper, and Nickel) and Body Centered Cubic (BCC) (Iron, Chromium, and Tungsten) metals to obtain the elastic modulus at a constant rate of loading using the Morse Potential. However, this study did not consider the effect of various potential types and did not compare to macroscale experimental results. In MD, the potential is required to determine the interatomic forces and accelerations between atoms; thus, allowing for realistic interactions between atoms and molecules during the simulation. Overall, there are several different types of many-body potentials. Depending on their purpose for development and specific parameterization, the potential being used may significantly affect simulation results. Recently, some studies [3]-[5] have tested mechanical properties using MD to investigate the accuracy of many-body potentials for iron, molybdenum, silicon, titanium, zirconium, and magnesium. However, there is little work testing the accuracy of various many-body potentials for FCC metals. Hence, the objective of the present study was to evaluate and compare accuracies amongst the various many-body potentials reflecting on their specific parameterizations in estimating the mechanical properties, elastic modulus, and Poisson ratio, of nanoscale FCC aluminum at room

temperature. Here, results are compared to experimental data [6] available for aluminum with crystal orientation <100>.

2.2. Molecular Dynamics

MD calculates the trajectories of atoms or molecules of a material using Newton's equation of motion, shown in Equation (2-1).

$$\vec{F} = m\vec{a} \tag{2-1}$$

Where $\vec{F}$ is the interatomic force between atoms or molecules, m is a constant mass of atoms or molecules, and $\vec{a}$ is the attractive or repulsive acceleration of atoms with other atoms. With initial positions and velocities known, the interatomic potential is used to calculate interatomic acceleration that defines the forces between interacting particles. Finally, the updated positions and velocities are then predicted using Equation (2-1). As such, potential type is a critical aspect of any simulation. The most commonly used many-body potentials, Embedded Atom Model (EAM), Modified EAM (MEAM), and Reactive Force Field (ReaxFF) were considered in the current study.

2.2.1. EAM and MEAM

Daw and Baskes [7] proposed the EAM potential to calculate several ground state properties, such as lattice constant, elastic constants, sublimation energy, and vacancy formation energy which were a limitation of pairwise potentials. Here, the EAM potential assumes that the interatomic potential is a function of the positions of all atoms and molecules in the simulation box. However, the directional bonding of the metals is the limitation of the EAM potential. In the EAM potential [8], the total energy of a monoatomic system is calculated by using Equations (2-2) and (2-3).

$$E_{tot} = \frac{1}{2}\sum_{ij} V(r_{ij}) + \sum_i F(\bar{\rho}_i) \quad (2\text{-}2)$$

Here $V(r_{ij})$ is a pair potential as a function of the distance r_{ij} between atoms *i* and *j*, and *F* is the embedding energy as a function of the host density ($\bar{\rho}_i$) induced at site *i* by all other atoms in the system. The host density is,

$$\bar{\rho}_i = \sum_{j \neq i} \rho(r_{ij}) \quad (2\text{-}3)$$

Where, $\rho(r_{ij})$ being the atomic density function.

In the present study, nine EAM potentials were used to predict an elastic modulus of single crystal aluminum. A discussion into the parameterization of the potentials is required to understand the accuracy of each potential. For the various many-body potentials utilized, parameterization and fitting varied with the different methods and sets of experimental data. For example, the Angelo *et al.* [9] EAM potential was fitted to study the effect of dislocations and grain boundaries on metal. In this study, data was trained to predict the defect energy because of trapped hydrogen in nickel and aluminum lattice. Next, the Liu *et al.* [10] EAM potential was parameterized using density functional theory to calculate improved stacking fault energy of aluminum. Generally, this potential was reliable to model crystal thermodynamics, and crystal defects. The Mendelev *et al.* [11] EAM potential was developed to reproduce melting properties and liquid structure of aluminum and copper. The Sturgeon *et al.* [12] EAM potential was the re-parameterization of the many-body potentials, which were generally optimized with respect to the mechanical properties where database was optimized at 0 K. The potential was used to calculate the melting temperature of aluminum. Here, the database was trained with experimental melting temperature without significantly

affecting the mechanical properties of aluminum. The Zhou *et al.* [13] EAM potential was developed to evaluate the lattice mismatch by calculating the formation of misfit-strain-reducing dislocation structures in vapor-deposited CoFe/NiFe multilayers. The Zope *et al.* [14] potential was developed for pure aluminum (Al), pure titanium (Ti) and TiAl system. For aluminum, the database was trained for lattice constant, cohesive energy, elastic constants, vacancy formation energy, and linear thermal-expansion factors at high temperatures (293-1000 K). The Winey *et al.* [15] EAM potential was proposed to determine the thermo-elastic response of aluminum. Here, atomic volume and the second- and third-order elastic constants measured at room temperature were extrapolated at 0 K using classical thermo-mechanical relations and then the interatomic potential is fitted to these 0 K pseudo-values, which were thermodynamically consistent in simulation. Hence, this enabled prediction of the correct thermo-mechanical response at temperatures near room temperature and higher. The Mishin *et al.* [8] EAM potential was parameterized by comparing the *ab initio* structural energies to those predicted by the potential. This strategy allows for a strong accuracy of fitting within the intrinsic limitations of the potential model. This potential accurately predicted the elastic constants, vacancy formation and migration energies, stacking fault energies, and surface energies for aluminum. Lastly, Sheng *et al.* [16] proposed a highly optimized EAM potential for fourteen FCC elements by fitting the potential-energy surface (PES) of each element derived from high-precision first-principles calculations. This potential was fitted against a comprehensive list of properties including lattice dynamics, mechanical properties, thermal behaviour, defects, deformation paths, and liquid structures.

To overcome the directional bonding limitation of the EAM potential, Baskes [17] proposed a new many-body potential, Modified EAM (MEAM). While the mathematical formulation of MEAM is the same as Equation (2-2) and (2-3), the MEAM potential adds an angle-dependent term to the embedding energy. Hence, the MEAM potential is commonly used for FCC, BCC, and Hexagonal close packed (HCP) crystal structures.

In this paper, three MEAM potentials were used to estimate the elastic modulus of single crystal aluminum. First, Dickel *et al.* [18] MEAM potential was proposed for zinc and various alloy system of Mg-Al-Zn. This potential was relaxed and trained for stable state, i.e. 0 K and the results were compared with experimental and DFT data for pure zinc and binary and ternary systems of Mg-Al-Zn. Second, the Al-U_Pascuet MEAM potential was developed to describe an Aluminum-Uranium (Al-U) interatomic alloy [19]. Here, the potential was fitted for thermo-elastic properties and point defects for this alloy. Finally, the Al_Pascuet MEAM potential was developed for pure aluminum and fitted with a database that included point defect properties, and the FCC elastic constants, vacancy and interstitial migration [19]. Here, the database for this potential was fully relaxed and optimized for 0 K.

2.2.2. ReaxFF

More recently, the ReaxFF [20], [21] potential was developed to model the chemical reactions and formation and breaking of bonds. This potential is highly dependent on bond order (i.e., valence, torsional angles) and bond types of the materials. The fundamental concept of this potential is that the bond strength between two atoms is not constant but depends on the local environment. Hence, the total energy term in the ReaxFF description is shown in Equation (2-4) [22].

$$E_{system} = E_{bond} + E_{over} + E_{under} + E_{lp} + E_{val} + E_{tors} + E_{vdWaals} + E_{Coulomb} \quad (2\text{-}4)$$

Where the total energy, E_{system} consists of the bond order dependent terms: the bond energy (E_{bond}), overcoordination (E_{over}), undercoordination (E_{under}), lone-pair (E_{lp}), valence angle (E_{val}), and torsion angle (E_{tors}). It also consists of the bond order independent terms, i.e., van der Waals energy ($E_{vdWaals}$) and Coulomb energy ($E_{Coulomb}$).

In this current study, two ReaxFF potentials were tested. First, Russo Jr *et al.* [23] reactive potential was proposed to investigate the dynamics associated with the dissociation of absorbed water molecules on an aluminum nanocluster surface. The database for this potential was parameterized with Quantum Mechanics (QM) and experimental results. This potential was developed for the study of a reactive metal/water system. Similarly, the other ReaxFF potential used in the present study, Hong *et al.* [22], was developed to investigate carbon coating and its effect on the oxidation of aluminum nanoparticles. Similar to the previous ReaxFF potential, this potential was optimized with QM and experimental data. Both ReaxFF potentials were developed for the study of chemical interaction between different molecules.

2.3. Materials and Methods

Utilising various many-body potentials from National Institute of Standards and Technology (NIST) interatomic repository [24], [25], a uniaxial tensile test at room temperature was simulated for single crystal aluminium using Large-scale Atomic/Molecular Massively Parallel Simulator (LAMMPS) [26]. Similar work to the work by Morrissey *et al.* [3] on pure iron, a 40.06 × 40.06 × 40.06 ($Å^3$) simulation box was first developed that contained 4000 atoms. The crystal orientation of the single crystal aluminum

was <1 0 0>, <0 1 0> and <0 0 1> in the x-, y- and z-directions, respectively. Here, loading was applied in the x-direction. Detailed input parameters for the simulation are provided in Table 2-1. For EAM and MEAM potentials, a time step for 1 Femtosecond (fs) was used. In contrast, the ReaxFF potential was trained for the different sets of units, hence the recommended time step for simulation was no larger than 0.5 fs [27]. Therefore, a time step of 0.25 fs was used for current study.

Table 2-1: Input parameters for LAMMPS simulations

	Potentials		
	EAM	**MEAM**	**ReaxFF**
Time step (fs)	1	1	0.25
Total Simulation time (fs)	2000	2000	8000
Strain rate (1/fs)	10^{-5}	10^{-5}	10^{-5}
Temperature damping factor	100	100	25
Pressure damping factor	1000	1000	250

For the equilibration, the simulation box was relaxed for 30 picoseconds by using a constant number, pressure, and temperature (NPT) ensemble to achieve the desired simulation temperature and density. During the equilibration, atoms fluctuated to attain the desired temperature by changing the simulation box dimensions as shown in Figure 2-1. After the system was equilibrated, the system was deformed uniaxially in the x-direction,

where the stress calculated was the negative pressure in the x-direction, calculated by Equation (2-5) below [28].

$$P_{ij} = \frac{\sum_k^N m_k v_{ki} v_{kj}}{V} + \frac{\sum_k^{N'} r_{ki} f_{kj}}{V} \tag{2-5}$$

where, *i,j* take the values of x, y, and z directions, *k* is the *k*th atom, *N* is the number of atoms in the system, m_k is mass of the *k*th atom, v_{ki} is the x-direction instantaneous velocity of the *k*th atom, v_{kj} is the y-direction instantaneous velocity of the *k*th atom, V is the system volume, r_{ki} is the instantaneous position vector of the *k*th atom, and f_{kj} is the total force acting on the *k*th atom [28].

The longitudinal strain was calculated as

$$\varepsilon_x = (\mathrm{L_x} - \mathrm{L_{x0}})/\mathrm{L_{x0}} \tag{2-6}$$

Where, the strain in loading direction is ε_x , $\mathrm{L_x}$ is the final length and $\mathrm{L_{x0}}$ is the original length of the simulation box in x-direction.

Similarly, the transverse strain was calculated as:

$$\varepsilon_y = (\mathrm{L_y} - \mathrm{L_{y0}})/\mathrm{L_{y0}} \tag{2-7}$$

Where, the strain in transverse direction is ε_y, L_y is the final length and L_{y0} is the original length of the simulation box in y-direction.

Hence, Poisson's ratio (ν) in the present simulation was calculated using

$$\nu = -\varepsilon_y/\varepsilon_x \tag{2-8}$$

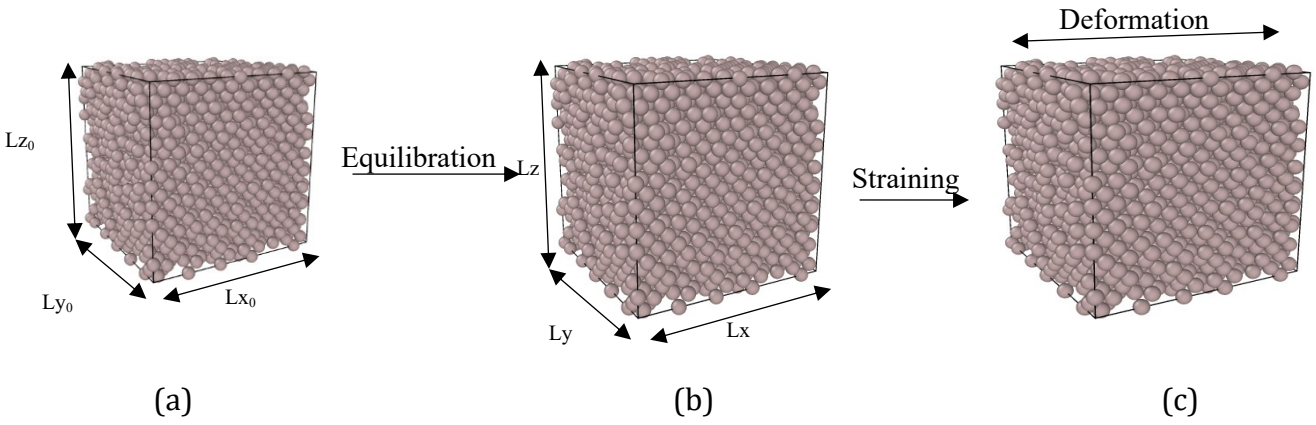

Figure 2-1: Simulation procedure for aluminum. (a) Initialization of the simulation box (b) Simulation box size changed after equilibration to adjust the temperature (c) Simulation box during the uniaxial tensile test. Here,Lx_0, Ly_0 and Lz_0 are the initialization length of the simulation box and Lx, Ly and Lz are the Equilibrated simulation box's lengths.

2.4. Results and Discussions

2.4.1. Effect of simulation box size

Different simulation box sizes were investigated to study the effect of box size on elastic modulus for single crystal aluminum. It was shown that there is a negligible effect of simulation box on the prediction of elastic modulus, Figure 2-2. Hence, the present simulations are independent of the simulation box size for the range considered. This is expected due to the periodic boundary conditions used and because strains were sampled in the elastic region.

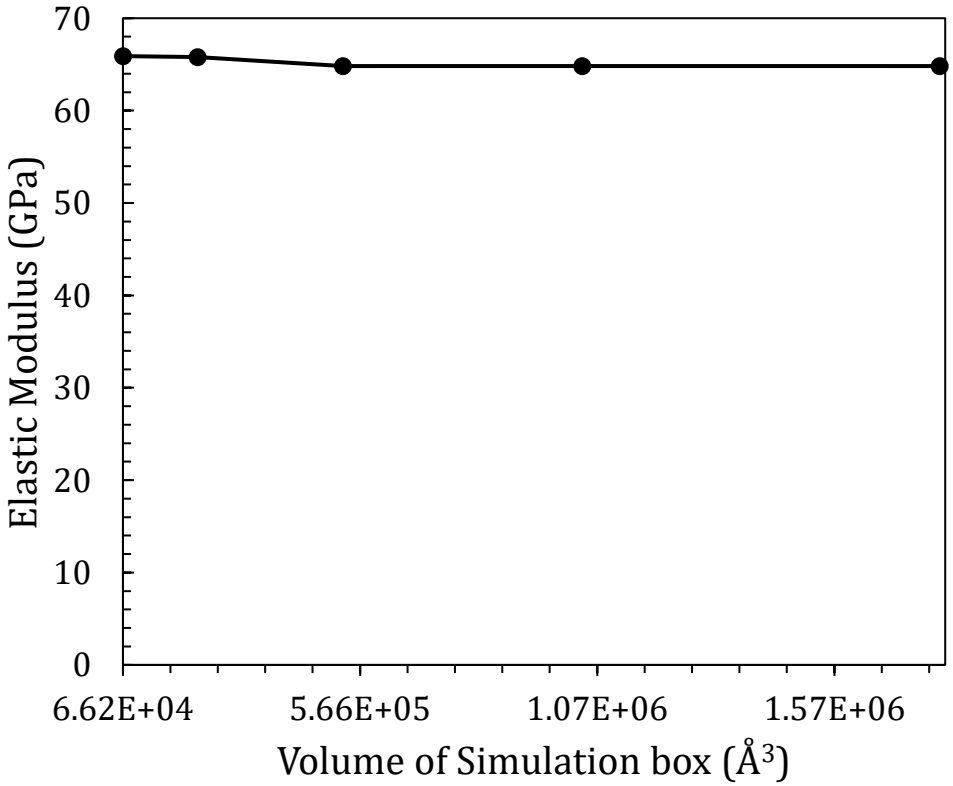

Figure 2-2: Investigation of the effect of simulation box size in estimating elastic modulus of Aluminum in MD simulation at 300 K using Sheng *et al.* [16] EAM potential.

2.4.2. Effect of strain rate

Similarly, strain rate is another important factor for tension tests. Therefore, the effect of various strain rates were compared in this study. Figure 2-3 shows that there is no effect of the strain rates while estimating elastic modulus for aluminum in MD tension test. Hence, the simulation and results are independent of the strain rates. This result agrees with the previous work of Yuan *et al.* [29] and Jensen *et al.* [30] who determined that the slope of the elastic region of a stress strain curve was independent of the strain rate considered.

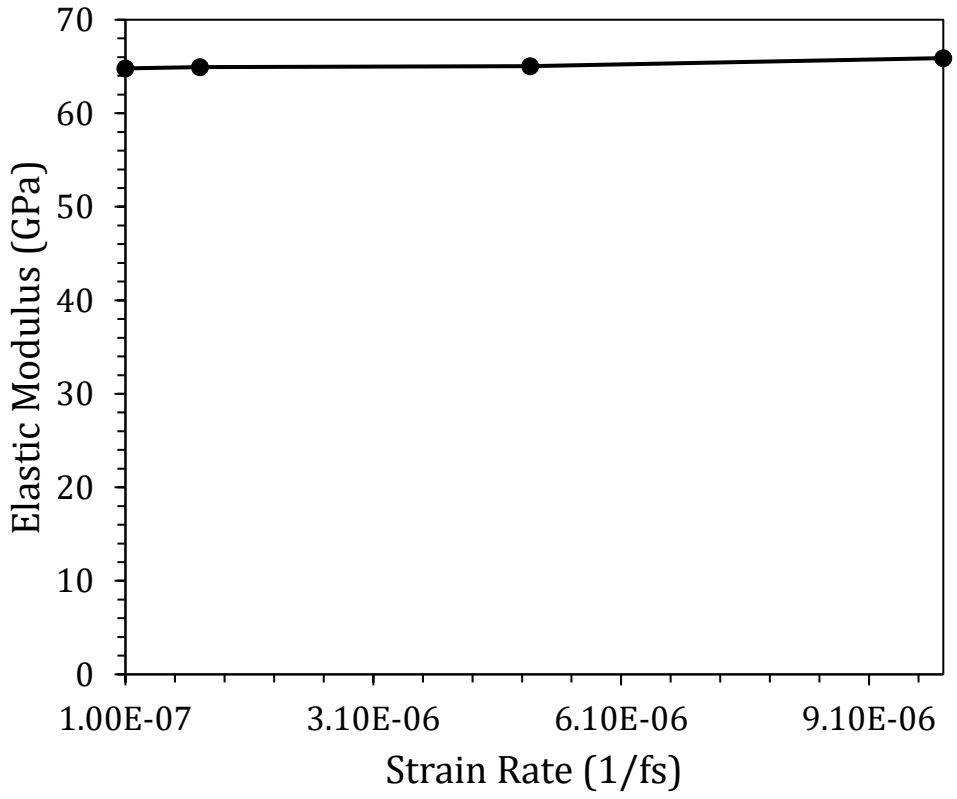

Figure 2-3: Investigation of the effect of strain rates in estimating elastic modulus of Aluminum in MD simulation at 300 K using Sheng *et al.* [16] EAM potential.

2.4.3. Elastic Modulus

The uniaxial tensile test was simulated in MD to capture the stress-strain behaviour of single crystal aluminum to compare the predicted elastic modulus from various many-body potentials. Here, strain rates for all simulations was kept constant (Table 2-1). In addition, total strains were kept to 2% to ensure calculation of the elastic modulus was performed within the linear region of the stress-strain curve where Hooke's law is applicable (Figures 2-4 - 2-6). The experimental data [6] was calculated by using an ultrasonic pulse technique for single crystal aluminum with crystal orientation <1 0 0> for various temperatures (4 to 300 K). A relation to be obtain the elastic modulus in various crystal orientations was provided by Zhang *et al.* [31]. This relation has been simplified to calculate the experimental elastic modulus for <1 0 0> crystal orientation in Equation 2-9 below.

$$E_{100} = 1/S_{11} \tag{2-9}$$

Where E_{100} is the elastic modulus for crystal orientation <1 0 0> and S_{11} is the elastic compliance for crystal orientation <1 0 0>.

Hence, Table 2-2 provides the comparison among various many-body potentials with the experimental data [6] for single crystal aluminum with crystal orientation <1 0 0>. Results for potentials with an accuracy within 5% are bolded.

Table 2-2: Comparison of the accuracy of the various many-body potentials with test results on estimating the elastic modulus of a single crystal Aluminum at crystal orientation [1 0 0]

Potentials name		Elastic Modulus (GPa)	
		Present Study	Error relative to single crystal Aluminium [1 0 0] (E=63.55 GPa[6])
EAM	Angelo *et al.* [9]	32.92	-48.20%
	Liu *et al.* [10]	88.22	38.82%
	Mendelev *et al.* [11]	51.35	-19.20%
	Sturgeon *et al.* [12]	39.09	-38.49%
	Zhou *et al.* [13]	23.41	-63.16%
	Zope *et al.* [14]	**60.57**	**-4.69%**
	Winey *et al.* [15]	**60.74**	**-4.42%**
	Mishin *et al.* [8]	**64.14**	**0.93%**
	Sheng *et al.* [16]	**65.41**	**2.93%**
MEAM	Dickel *et al.* [18]	58.89	-7.33%
	Al-U_Pascuet *et al.* [19]	57.64	-9.30%
	Al_Pascuet *et al.* [19]	58.45	-8.03%
ReaxFF	Russo Jr *et al.* [23]	98.37	54.79%
	Hong *et al.* [22]	40.57	-36.16%

2.4.3.1. EAM

In the present study, nine EAM potentials were used in estimating the elastic modulus of aluminum. Stress-strain curves for the EAM potentials are shown in Figure 4. In addition, the comparisons of the elastic modulus obtained from Figure 2-4 with experimental data are provided listed in Table 2-2. Predicted elastic modulus for EAM potentials was in the range of 23.41 to 88.22 GPa. Here, Liu *et al.* [10] over-predicted whereas Zhou *et al.* [13] under-predicted the elastic modulus for single crystal aluminum. As mention in parameterization prior, the Liu *et al.* [10] EAM potential was trained for crystal thermodynamics and crystal defects whereas Zhou *et al.* [13] EAM potential was parameterized for the lattice mismatch of the system. Further, Mendelev *et al.* [11], Strugeon *et al.* [12] and Angelo *et al.* [9] EAM potential under-predicted elastic modulus of aluminum. As described prior, Mendelev *et al.* [11] and Strugeon *et al.* [12] EAM potentials were optimized to reproduce melting properties of aluminum while the Angelo *et al.* [9] EAM potential was trained for the calculation of defect energy of trapped hydrogen in aluminum lattice. None of the above potentials were parameterized for elastic constants at room temperature; thus leading to a lack of accuracy when compared to the experimental results [6]. Conversely, the Zope *et al.* [14], Winey *et al.* [15], Mishin *et al.* [8], and Sheng *et al.* [16] EAM potentials predicted a highly accurate elastic modulus, in the range of 60.5-65.4 GPa. From Figure 2-4, the stress-strain curves for these four potentials were very close and relative error when comparing with experimental data [6] was between 0.93-4.69%. The database for these four potentials were well trained for elastic constants for aluminum at room temperature. Hence, these potentials show excellent agreement in predicting elastic modulus when compared with experimental data [6]. Of these four, the Mishin *et al.* [8] potential was most accurate with 0.93% relative error.

However, the stresses estimated were significantly higher due to the length scale limitation of MD simulations, the present simulation was focused to calculate elastic modulus from the slope of the curve.

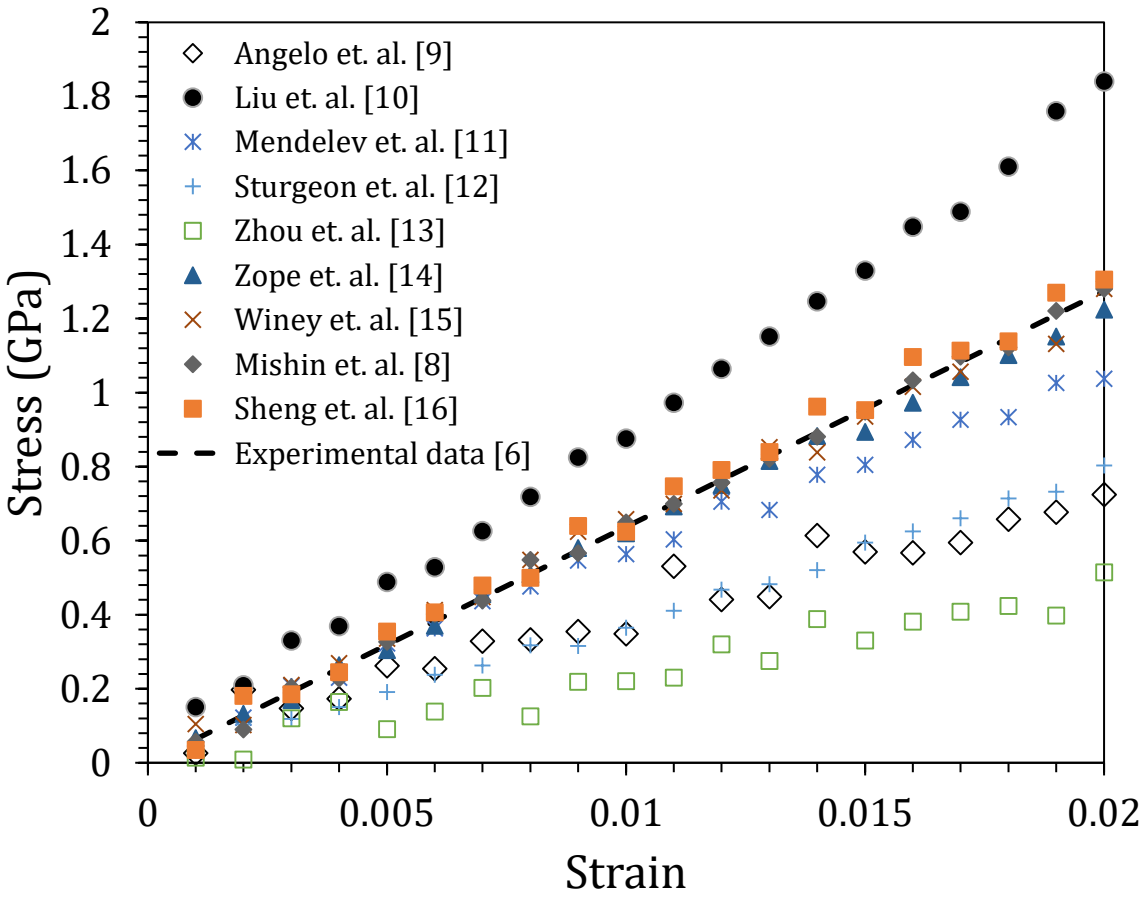

Figure 2-4: Stress-strain curves for different EAM potentials at 300 K.

2.4.3.2. MEAM

In current study, three MEAM potentials were used to estimate the elastic modulus of single crystal aluminum. From Table 2-2, the elastic modulus predicted using these potentials was in the range of 57-59 GPa. In addition, the stress-strain curve for these three potentials follow an almost identical trend (Figure 2-5). However, the potential specific

parameterizations can be used to shed light on the relative error. First, Dickel *et al.* [18] data was optimized at 0 K for pure zinc and an alloy system of Mg-Al-Zn. Therefore, no mention was made of pure aluminum and this potential thus under-predicted results when compared with experimental data [6] at room temperature. Similarly, Al-U_Pascuet *et al.* and Al_Pascuet *et al.* MEAM potentials [19] were parameterized and optimized at 0 K. This temperature is not physically realizable and cannot be used to extrapolate to the room temperatures typically found in experimental tests. As such, all of the MEAM potentials under-predicted elastic modulus due to the lack of parameterization to elastic constants at realizable temperatures.

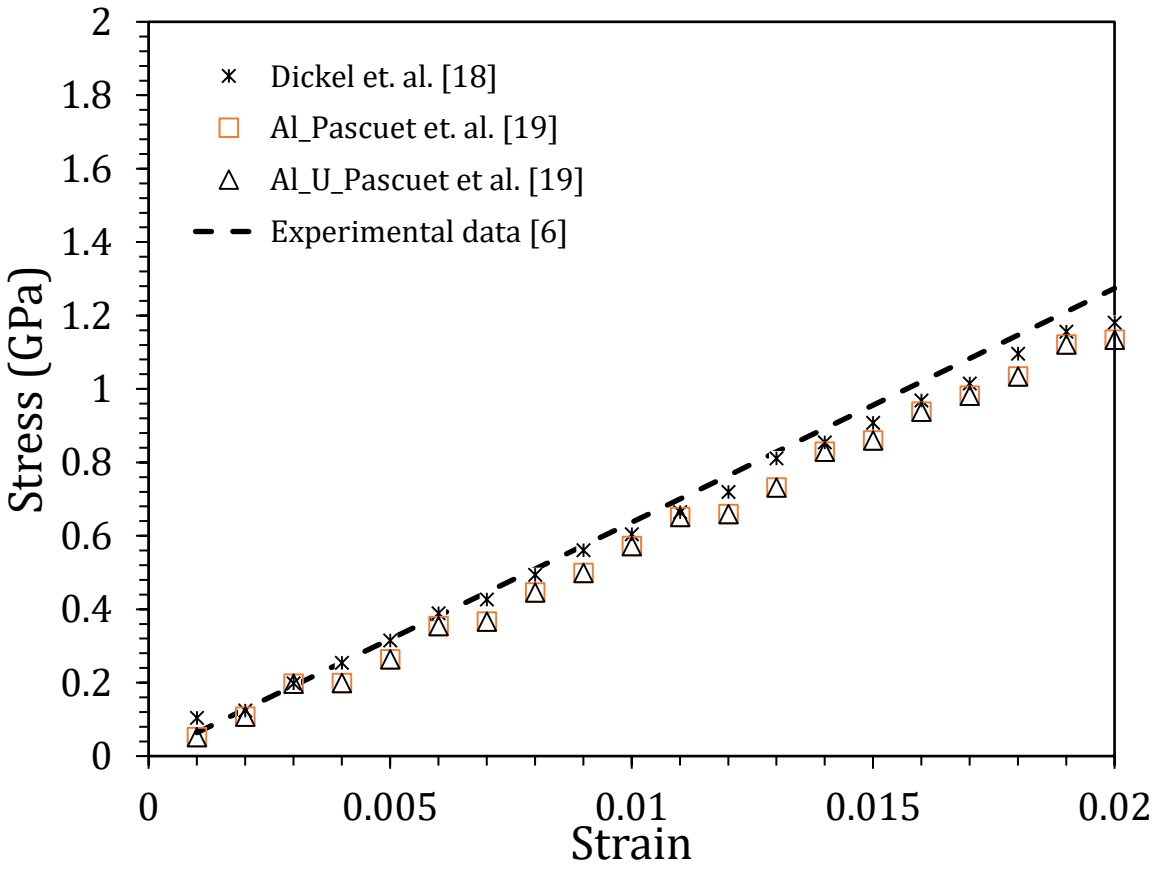

Figure 2-5: Stress strain curves for different MEAM potentials at 300 K

2.4.3.3. ReaxFF

Lastly, two ReaxFF potentials were tested in this current research. As mentioned prior, both ReaxFF potentials, Russo Jr *et al.* [23] and Hong *et al.* [22], were optimized with QM and experimental data and no parameterisation was conducted with elastic properties of aluminum since the primary objective of these potentials were to investigate the chemical reaction between aluminum and other molecules. Hence, the estimation of elastic modulus for single crystal aluminum was not intended for these potentials and error was significant.

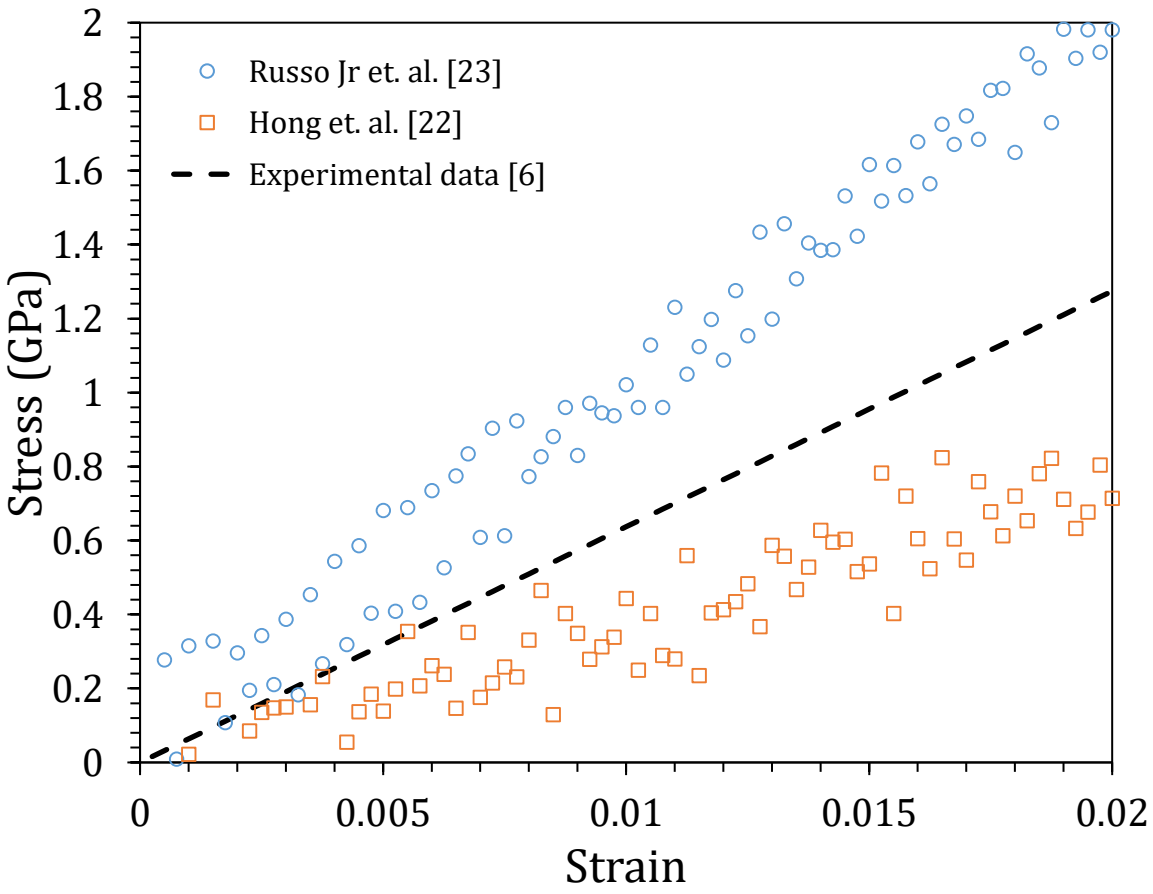

Figure 2-6: Stress strain curves for different ReaxFF potentials at 300 K

2.4.3.4. Importance of Potential Parameterization

As shown in the above review, depending on the potential used there is a wide range of predicted values for elastic modulus. Moreover, no one specific potentials type was necessarily more accurate. Instead, it is critical to interrogate the potential specific parameterization procedures prior to application. As demonstrated in the present study, those potentials parameterized with elastic constants at physically realizable temperatures consistently showed the highest accuracy as compared to experimental values. In each of these studies, elastic constants were obtained using a triaxial static method to apply stress. In other words, even though they were not directly tested for the uniaxial stress case, they still showed the highest accuracy. In contrast, those potentials that did not consider elastic constants or parameterized at 0K were consistently less accurate.

2.4.4. Poisson's Ratio

After completing the analysis into the elastic modulus, an investigation into the Poisson's ratio was completed to allow for complete material classification. Here, Poisson's ratio was calculated for all fourteen interatomic potentials and a quantitative comparison was performed with test data [6]. A relation to be obtain the Poisson's ratio in various crystal orientations for a cubic metal was provided by Zhang *et al.* [31]. This relation has been simplified to calculate the experimental Poisson's ratio for <1 0 0> crystal orientation in Equation (2-10) below.

$$\nu_{100} = S_{12}/-S_{11} \tag{2-10}$$

Where ν_{100} is the Poisson's ratio for crystal orientation <1 0 0>, and S_{11} and S_{12} are the elastic compliance for crystal orientation <1 0 0>.

Results are provided in Table 2-3. From Table 2-3, all fourteen interatomic potentials have relative error between 1% to 20%. Therefore, the range of error for Poisson's ratio was much smaller than observed for the elastic modulus. This suggests that even if a potential is inaccurate in calculating an elastic modulus, it still may be able to capture the relative lateral deformations with reasonable accuracy. Among the fourteen interatomic potentials, those that were most accurate for elastic modulus also showed the highest accuracy in Poisson's ratio. The Mishin et al. [8], and Sheng *et al.* [16], show good agreement [relative error = 1% - 5%] in estimating Poisson's ratio with the test data. However, like for the prediction of elastic modulus, the Mishin et al. [8] potential was the most accurate for predicting Poisson's ratio.

Table 2-3: Comparison of the accuracy of the various many-body potentials with test results on estimating the Poisson's ratio of a single crystal Aluminum at crystal orientation [1 0 0]

	Potentials name	Poisson's Ratio	
		Present Study	Error relative to single crystal Aluminium [1 0 0] **(ν=0.362) [6]**
EAM	Angelo *et al.* [9]	0.292	-19.34%
	Liu *et al.* [10]	0.334	-7.73%
	Mendelev *et al.* [11]	0.339	-6.35%
	Sturgeon *et al.* [12]	0.386	6.63%
	Zhou *et al.* [13]	0.387	6.91%
	Zope *et al.* [14]	**0.33**	**-8.84%**
	Winey *et al.* [15]	**0.327**	**-9.67%**
	Mishin *et al.* [8]	**0.369**	**1.93%**
	Sheng *et al.* [16]	**0.345**	**-4.70%**
MEAM	Dickel *et al.* [18]	0.354	-2.21%
	Al-U_Pascuet *et al.* [19]	0.309	-14.64%
	Al_Pascuet *et al.* [19]	0.349	-3.59%
ReaxFF	Russo Jr *et al.* [23]	0.327	-9.67%
	Hong *et al.* [22]	0.407	12.43%

2.5. Conclusion

In the present study, a uniaxial tensile test using molecular dynamics simulation was performed at room temperature to estimate the elastic modulus and Poisson's ratio for single crystal aluminum. The results were compared with experimental test data to investigate the ability of various many-body potentials to evaluate accurate elastic modulus and Poisson's ratio. In total, fourteen interatomic potentials were tested. It was demonstrated that parameterization of the potential highly influenced the prediction of both elastic modulus and Poisson's ratio. Potentials fitted and parameterized for elastic constants at room temperature demonstrated the highest accuracy, while potentials which lacked these parameterizations were less accurate. The most accurate potentials tested was the EAM Mishin et al. potential with an error less than 1%. Future work will extend these findings beyond single element/single crystal systems to binary systems and nanocrystalline structures. As such, the most accurate potentials for investigating the elastic modulus and Poisson's ratio of single crystal aluminum are provided within the present study.

References

1. Schiøtz, J., Vegge, T., Di Tolla, F. D., and Jacobsen, K. W. (1999). Atomic-scale simulations of the mechanical deformation of nanocrystalline metals. *Physical Review B*, *60*(17), 11971.
2. Komanduri, R., Chandrasekaran, N., and Raff, L. M. (2001). Molecular dynamics (MD) simulation of uniaxial tension of some single-crystal cubic metals at nanolevel. *International Journal of Mechanical Sciences*, *43*(10), 2237-2260.
3. Morrissey, L. S., Handrigan, S. M., Subedi, S., and Nakhla, S. (2019). Atomistic uniaxial tension tests: investigating various many-body potentials for their ability to produce accurate stress strain curves using molecular dynamics simulations. *Molecular Simulation*, *45*(6), 501-508.
4. Etesami, S. A., Laradji, M., and Asadi, E. (2018). Interatomic potentials transferability in predicting temperature dependency of elastic constants for titanium, zirconium and magnesium. *Modelling and Simulation in Materials Science and Engineering*.
5. Lysogorskiy, Y. V., Hammerschmidt, T., Janssen, J., Neugebauer, J., and Drautz, R. (2019). Transferability of interatomic potentials for molybdenum and silicon. *Modelling and Simulation in Materials Science and Engineering*.
6. Vallin, J., Mongy, M., Salama, K., and Beckman, O. (1964). Elastic constants of aluminum. *Journal of Applied Physics*, *35*(6), 1825-1826.
7. Daw, M. S., and Baskes, M. I. (1984). Embedded-atom method: Derivation and application to impurities, surfaces, and other defects in metals. *Physical Review B*, *29*(12), 6443.

8. Mishin, Y., Farkas, D., Mehl, M. J., and Papaconstantopoulos, D. A. (1999). Interatomic potentials for monoatomic metals from experimental data and ab initio calculations. *Physical Review B*, *59*(5), 3393.
9. Angelo, J. E., Moody, N. R., and Baskes, M. I. (1995). Trapping of hydrogen to lattice defects in nickel. *Modelling and Simulation in Materials Science and Engineering*, *3*(3), 289.
10. Liu, X. Y., Ercolessi, F., and Adams, J. B. (2004). Aluminium interatomic potential from density functional theory calculations with improved stacking fault energy. *Modelling and Simulation in Materials Science and Engineering*, *12*(4), 665.
11. Mendelev, M. I., Kramer, M. J., Becker, C. A., and Asta, M. (2008). Analysis of semi-empirical interatomic potentials appropriate for simulation of crystalline and liquid Al and Cu. *Philosophical Magazine*, *88*(12), 1723-1750.
12. Sturgeon, J. B., and Laird, B. B. (2000). Adjusting the melting point of a model system via Gibbs-Duhem integration: Application to a model of aluminum. *Physical Review B*, *62*(22), 14720.
13. Zhou, X. W., Johnson, R. A., and Wadley, H. N. G. (2004). Misfit-energy-increasing dislocations in vapor-deposited CoFe/NiFe multilayers. *Physical Review B*, *69*(14), 144113.
14. Zope, R. R., and Mishin, Y. (2003). Interatomic potentials for atomistic simulations of the Ti-Al system. *Physical Review B*, *68*(2), 024102.
15. Winey, J. M., Kubota, A., and Gupta, Y. M. (2009). A thermodynamic approach to determine accurate potentials for molecular dynamics simulations: thermoelastic

response of aluminum. *Modelling and Simulation in Materials Science and Engineering*, *17*(5), 055004.

16. Sheng, H. W., Kramer, M. J., Cadien, A., Fujita, T., and Chen, M. W. (2011). Highly optimized embedded-atom-method potentials for fourteen fcc metals. *Physical Review B*, *83*(13), 134118.
17. Baskes, M. I. (1992). Modified embedded-atom potentials for cubic materials and impurities. *Physical review B*, *46*(5), 2727.
18. Dickel, D. E., Baskes, M. I., Aslam, I., and Barrett, C. D. (2018). New interatomic potential for Mg–Al–Zn alloys with specific application to dilute Mg-based alloys. *Modelling and Simulation in Materials Science and Engineering*, *26*(4), 045010.
19. Pascuet, M. I., and Fernández, J. R. (2015). Atomic interaction of the MEAM type for the study of intermetallics in the Al–U alloy. *Journal of Nuclear Materials*, *467*, 229-239.
20. Nielson, K. D., Van Duin, A. C., Oxgaard, J., Deng, W. Q., and Goddard, W. A. (2005). Development of the ReaxFF reactive force field for describing transition metal catalyzed reactions, with application to the initial stages of the catalytic formation of carbon nanotubes. *The Journal of Physical Chemistry A*, *109*(3), 493-499.
21. Van Duin, A. C., Dasgupta, S., Lorant, F., and Goddard, W. A. (2001). ReaxFF: a reactive force field for hydrocarbons. *The Journal of Physical Chemistry A*, *105*(41), 9396-9409.
22. Hong, S., and van Duin, A. C. (2016). Atomistic-scale analysis of carbon coating and its effect on the oxidation of aluminum nanoparticles by ReaxFF-molecular dynamics simulations. *The Journal of Physical Chemistry C*, *120*(17), 9464-9474.

23. Russo Jr, M. F., Li, R., Mench, M., and Van Duin, A. C. (2011). Molecular dynamic simulation of aluminum–water reactions using the ReaxFF reactive force field. *International Journal of Hydrogen Energy*, *36*(10), 5828-5835.
24. Becker, C. A., Tavazza, F., Trautt, Z. T., and de Macedo, R. A. B. (2013). Considerations for choosing and using force fields and interatomic potentials in materials science and engineering. *Current Opinion in Solid State and Materials Science*, *17*(6), 277-283.
25. Hale, L. M., Trautt, Z. T., and Becker, C. A. (2018). Evaluating variability with atomistic simulations: the effect of potential and calculation methodology on the modeling of lattice and elastic constants. *Modelling and Simulation in Materials Science and Engineering*, *26*(5), 055003.
26. Plimpton, S. (1995). Fast parallel algorithms for short-range molecular dynamics. *Journal of computational physics*, *117*(1), 1-19.
27. van Duin, A. (2002). Reaxff user manual. *California Institute of Technology, Materials and Process Simulation Center*.
28. Thompson, A. P., Plimpton, S. J., and Mattson, W. (2009). General formulation of pressure and stress tensor for arbitrary many-body interaction potentials under periodic boundary conditions. *The Journal of chemical physics*, *131*(15), 154107.
29. Yuan, F., and Huang, L. (2012). Molecular dynamics simulation of amorphous silica under uniaxial tension: From bulk to nanowire. *Journal of Non-Crystalline Solids*, *358*(24), 3481-3487.
30. Jensen, B. D., Wise, K. E., and Odegard, G. M. (2015). The effect of time step, thermostat, and strain rate on ReaxFF simulations of mechanical failure in diamond, graphene, and carbon nanotube. *Journal of computational chemistry*, *36*(21), 1587-1596.

31. Zhang, J. M., Zhang, Y., Xu, K. W., and Ji, V. (2007). Young's modulus surface and Poisson's ratio curve for cubic metals. *Journal of Physics and Chemistry of Solids*, *68*(4), 503-510.

3. Chapter 3: Mechanical Properties of Nanocrystalline Aluminum: A Molecular Dynamics Investigation

Abstract:

Uniaxial deformation was performed using molecular dynamics to estimate the mechanical properties of nanocrystalline aluminum. It was observed that the stacking faults and sliding of the grain boundaries affected the mechanical properties. In addition, nucleation of atoms near grain boundaries during deformation hardened the nanocrystalline material as the grain diameter increased (Hall-Petch relation). Further, the effects of strain rate and temperature were investigated with various mean grain diameters. Investigation showed that mechanical properties are independent of strain rates (10^{9}-10^{10} s^{-1}) and that the nanocrystalline material softened with increasing temperature. The elastic modulus and Poisson's ratio were then compared to experimental results from literature at room temperature.

3.1. Introduction

In recent years, engineers and researchers are highly interested in understanding the mechanical behavior of nanocrystalline materials due to their potential industrial applications. Suryanarayana [2] discussed the importance of nanocrystalline materials in real world applications, providing a comprehensive review of structural and mechanical properties of various nanocrystalline materials. In addition, the author highlighted the applications of nanocrystalline materials in industries such as high-efficiency gas turbines, aerospace, and automotive components, where aluminum is a major constituent of many of these structures. Due to the difficulty and costs associated with producing nanocrystalline

materials, a more efficient method of analysis is required. As a result, many researchers are utilizing Molecular Dynamics (MD) simulations to study such materials.

Schiotz et al. [1] performed a uniaxial tensile test in atomistic-scale simulations using the Effective Medium Theory (EMT) potential [3] for a nanocrystalline copper and investigated the elastic and plastic behavior. They considered the effect of various strain rates and temperatures on the stress-strain response. Findings demonstrated that the sliding of grain boundaries in the simulation box affected the elastic and plastic deformation of the nanocrystalline copper. The study concluded that this phenomenon affected the elastic modulus since modulus was under-predicted when compared with experimental data for polycrystalline copper. Schiotz also observed a reverse Hall-Petch relationship – hardness increased with increasing grain size. Building on these findings, Schiotz et al. [4] briefly described the softening of a nanocrystalline metal at various grain size at room temperature while comparing with bulk copper.

Similar work has been performed on other materials, such as aluminum. For example, Xu et al. [5] carried out classical MD simulations of the uniaxial tensile deformation of nanocrystalline aluminum with various grain sizes using the Mishin et al. [6] Embedded Atom Method (EAM) potential at a strain rate of 10^{10} per second. The atomic fraction of dislocations and reverse Hall-Petch relation were investigated. However, the effect of strain rate on mechanical properties was not studied. In addition, there were not any clear comparisons of elastic modulus and Poisson's ratio with experimental data. Likewise, Kadau et al. [7] performed tensile loading of nanocrystalline aluminum in large-scale molecular dynamics simulation using an EAM potential. Two different sample preparation methods

were compared, namely the Voronoi construction and sintered method. Kadau et al. described similar trends for the reverse Hall-Petch relation on nanocrystalline aluminum to those observed by Schiotz et al. [1] for nanocrystalline copper. However, Kadau et al. did not investigate the elastic modulus and Poisson's ratio, nor did they investigate the effect of temperature and strain rate.

As discussed, previous studies have investigated the mechanical deformation of nanocrystalline aluminum. However, these studies did not consider the elastic modulus or Poisson's ratio. They also did not investigate the effect of strain rate or temperature on these properties. As well, the studies lack comparisons to experimental results in order to validate findings. Therefore, to close this knowledge gap, the current study investigated the effect of strain rate, grain size, and temperature on predicting elastic modulus and Poisson's ratio of nanocrystalline aluminum. To verify to the accuracy of the findings, results were then compared to experimental data from literature ([16] and [26]) for nano-crystalline aluminum.

3.2. Molecular Dynamics

MD involves simulating the interactions of atoms and molecules to predict material properties via atomic velocities and acceleration. Here, the interatomic acceleration is determined using a potential, which describes the interatomic force based on the initial atomic positions. Using this acceleration, the final velocities and positons of the interacting atoms are determined. In the present study, the most commonly used many-body potential, Mishin et al. [6] EAM potential, is considered.

3.2.1. Mishin et al. EAM potential

In the present study, the Mishin et al. EAM potential was used to predict an elastic modulus of nanocrystalline aluminum. The EAM potential is a function of the positions of the interacting particles. Since this potential was developed with a single fitting procedure, it is less complicated and a better option for uniformly bonded materials, such as aluminum [9]. For the formulation of the EAM potential [6], Equations (3-1) and (3-2) are used to calculate the total energy of a monoatomic system.

$$E_{tot} = \frac{1}{2}\sum_{ij} V(r_{ij}) + \sum_i F(\bar{\rho}_i) \tag{3-1}$$

Here $V(r_{ij})$ is a pair potential as a function of the distance r_{ij} between atoms, *i* and *j*, and *F* is the embedding energy as a function of the host density ($\bar{\rho}_i$) induced at site *i* by all other atoms in the system. The host density is,

$$\bar{\rho}_i = \sum_{j \neq i} \rho(r_{ij}) \tag{3-2}$$

where, $\rho(r_{ij})$ being the atomic density function.

During development, the Mishin et al. potential was parameterized to accurately predict the elastic constants, vacancy formation, migration energies, stacking fault energies, and surface energies for aluminum. Previous research has demonstrated that the interatomic potential can significantly affect the predicted elastic modulus in uniaxial tension tests [21-24]. In an assessment of available potential for aluminum, Subedi et al. [24] demonstrated that the Mishin potential had the highest accuracy of potentials tested when predicting single crystal

aluminum elastic modulus at 300K. Therefore, this potential was chosen for the nanocrystalline simulations.

3.2.2. Construction of simulation box

Utilizing the open-source code, Atomsk [10], a nanocrystalline aluminum structure was constructed with randomly oriented grains. The structure was produced using Voronoi Construction [7, 11-14]. In Voronoi Construction [7], grain centers are randomly distributed and each center is assigned a lattice orientation. Next, grain boundaries are created around these grain centers in random fashion. Afterwards, using an FCC unit cell of aluminum as a seed, atoms are added to each grain according to the grain's lattice orientation. Periodic boundary conditions were considered during construction of the computational cell. Here, the grains were equiaxed and divided by narrow grain boundaries. Three different randomly oriented structures for each mean grain diameter were utilized in the current study to obtain average properties.

3.3. Numerical Procedure

In the present study, the Mishin et al. [6] EAM potential was obtained from National Institute of Standards and Technology (NIST) interatomic repository [17-18]. Using this potential, a uniaxial tensile test was simulated for nanocrystalline aluminum using Large-scale Atomic/Molecular Massively Parallel Simulator (LAMMPS) [19] at various temperatures (50K-500K). A 200 × 200 × 200 ($Å^3$) simulation box was constructed using Voronoi Construction with different grain sizes ranging from 4.29 to 13.82 nm. Table 3-1 shows the number of randomly oriented grains in the simulation box and their corresponding grain diameters. Here, the simulation box contained approximately 500,000

atoms, which were oriented in different crystal structures, i.e. FCC, BCC, HCP and others. The grain boundaries included BCC, HCP and other crystal structures and the atoms inside the grain boundary were FCC structured as shown in Figure 3-1.

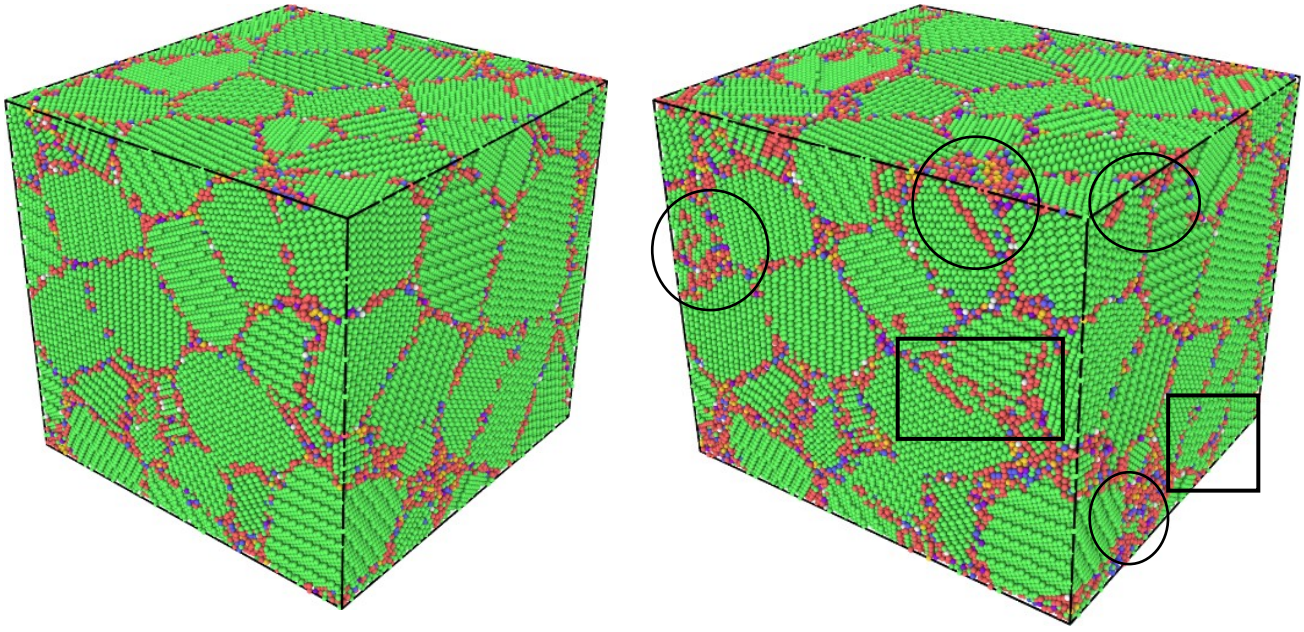

(a) (b)

Figure 3-1: The equilibrated simulation box for a nanocrystalline Aluminum at 300 K (a) at initial, and (b) after 10% strain. The system contains 500,000 atoms arranged in 48 grains with an average grain diameter 6.91 nm. Green colored atoms are in perfect FCC structure, Red atoms are in HCP structure and Blue atoms are other structured atoms. Black circles show the nucleation of atoms near grain boundaries and black rectangles show the formation of dislocations in the system.

Table 3-1: Mean grain diameter for the respective number of grains in the simulation box.

Number of grains	**Mean Grain diameter (nm)**
6	13.82
12	10.97
48	6.91
100	5.41
200	4.29

During equilibration, the NPT ensemble was used to allow the simulation box to attain the desired temperature. In the NPT ensemble [19], Nose/Hoover temperature thermostat and Nose/Hoover pressure barostats are used to create a system trajectory consistent with the isothermal-isobaric ensemble. After equilibration, the simulation box was deformed to 10% of the total length in the x-direction. Table 3-2 provides the input parameters for the numerical simulation for various strain rates.

Table 3-2: Parameters used for simulations

	EAM Potential
Time step (fs)	1
Total Simulation time (fs)	10^4-10^5
Strain rate (1/s)	10^9-10^{10}
Temperature damping factor	100
Pressure damping factor	1000

Stresses were calculated using virial stress tensor that is calculated, using Equation (3-3), as described by Thompson et al. [20]. This has been shown to be equivalent to macroscale continuum stress [27].

$$P_{ij} = \frac{\sum_k^N m_k v_{ki} v_{kj}}{V} + \frac{\sum_k^{N'} r_{ki} f_{kj}}{V} \tag{3-3}$$

where, *i, j* take the values of x, y, and z directions, *k* is the *k*th atom, *N* is the number of atoms in the system, m_k is a mass of the *k*th atom, v_{ki} is the x-direction instantaneous velocity of the *k*th atom, v_{kj} is the y-direction instantaneous velocity of the *k*th atom, V is the system volume, r_{ki} is the instantaneous position vector of the *k*th atom, and f_{kj} is the total force acting on the *k*th atom [20].

As the simulation box was deformed in the x-axis, the longitudinal strain and the transverse strain were calculated using Equations (3-4) and (3-5), respectively.

$$\varepsilon_x = (\mathrm{L_x} - \mathrm{L_{x0}})/\mathrm{L_{x0}} \tag{3-4}$$

$$\varepsilon_y = (\mathrm{L_y} - \mathrm{L_{y0}})/\mathrm{L_{y0}} \tag{3-5}$$

where the strain in loading direction is ε_x , $\mathrm{L_x}$ is the final length, and $\mathrm{L_{x0}}$ is the original length of the simulation box in x-direction. Similarly, for the y-direction, the strain in transverse direction is ε_y, $\mathrm{L_y}$ is the final length, and $\mathrm{L_{y0}}$ is the original length of the simulation box in y-direction.

Using Equations (3-4) and (3-5), Poisson's ratio (ν) for the simulation box was calculated using Equation (3-6).

$$\nu = -\varepsilon_y/\varepsilon_x \tag{3-6}$$

The validation of the numerical procedure is shown in Appendix 1.

3.4. Results and Discussions

3.4.1. Effect of strain rate on estimating mechanical properties

To investigate the effect of strain rate, the mean grain size and temperature were held constant. A mean grain size of 6.91 nm was investigated at 300K. Similar to the work of Schiotz et al [1], various strain rates ranging from 10^9 to 10^{10} s^{-1} were used to deform a nanocrystalline aluminum structure. The dependence of mechanical properties on strain rate is shown in Figures 3-2 and 3-3. From the stress-strain curves, the elastic moduli were determined within the linear region (ε = 2%). The elastic modulus obtained in this investigation ranged from 48.65 to 53.65 GPa. For the strain rates used in the current study,

the difference in elastic modulus is minimal as shown in Figure 3-2. Poisson's ratio was also investigated for various strain rates and plotted in Figure 3-3. The Poisson's ratio curve follows a similar trend as elastic moduli curve. Similar to the work of Xu et al. [5] who also simulated nanocrystalline aluminum, a strain rate of 10^{10} s^{-1} was chosen in the current study to reduce the computational demand of the simulations.

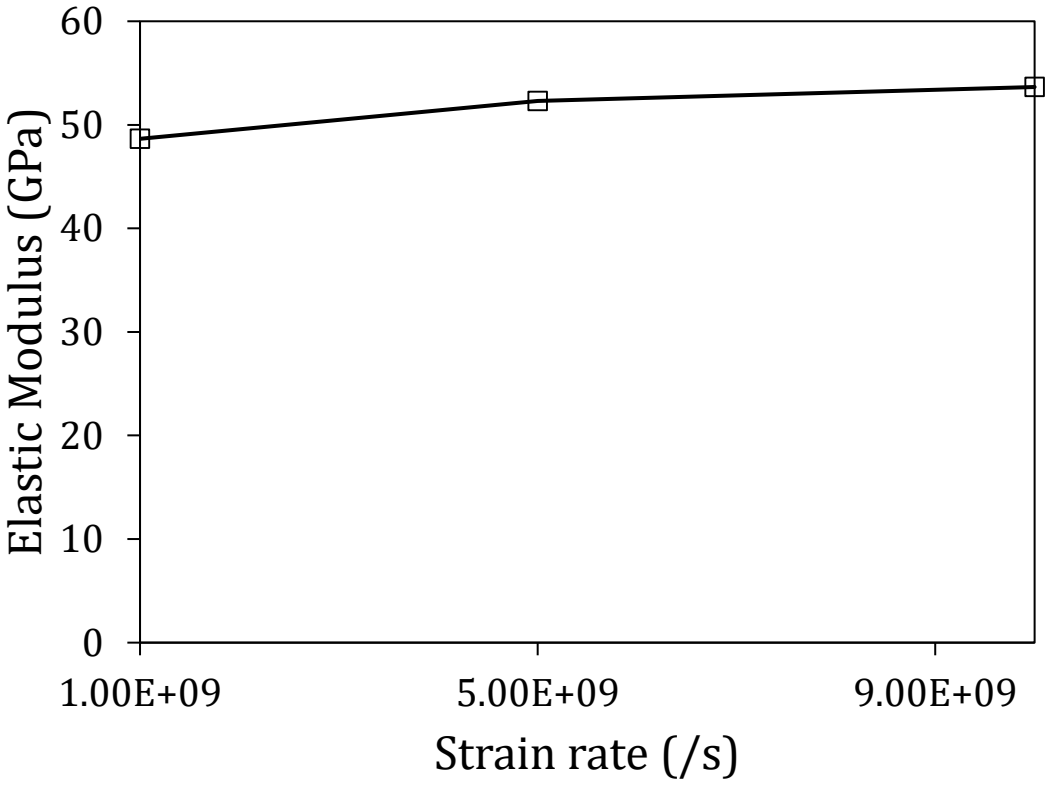

Figure 3-2: Effect of strain rates on elastic modulus for a nanocrystalline aluminum with average grain boundary 6.91 nm at 300K.

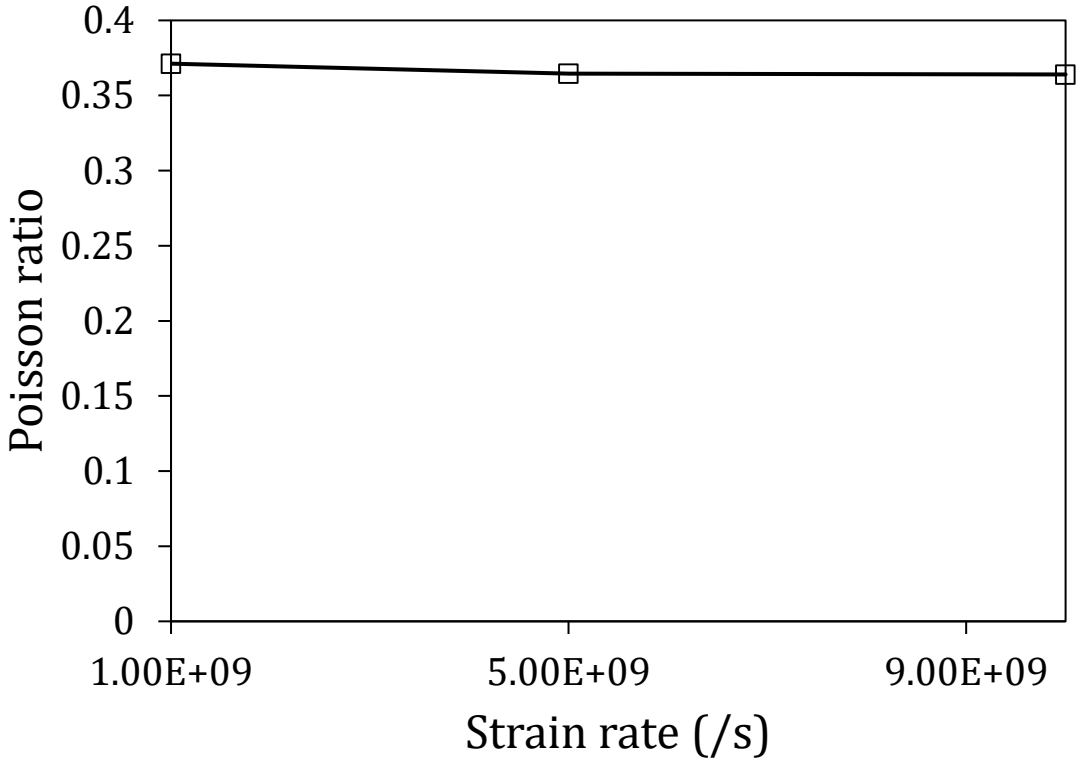

Figure 3-3: Effect of strain rates on Poisson's ratio for a nanocrystalline aluminum with average grain boundary 6.91 nm at 300K.

3.4.2. Effect of grain size on estimating mechanical properties

With the strain rate chosen, the next step was to investigate the effect of grain size on estimating the mechanical properties. While significant literature exists to describe the microstructure of nanocrystalline aluminum, few literatures include the associated mechanical properties. One study of interest by Haque et al. [16] performed an experimental uniaxial tensile test for a nanocrystalline aluminum with the grain size 11.1 nm. The results obtained from the current study were compared with the experimental data from Haque et al. [16]. In addition, a comparison of single crystal moduli is shown with additional experimental data [26] to further justify the potential's accuracy. This comparison is shown

in Table 3-3. Here, the relative error for single crystal aluminum to the experimental results is 0.93% whereas for a nanocrystalline aluminum with mean grain size 11.1 nm the relative error is 4.45%. Hence, the authors are confident in the prediction of mechanical properties of nanocrystalline aluminum utilizing MD paired with the Mishin et al. potential.

Table 3-3: Comparison of the elastic modulus obtained from molecular simulation with experimental results

Aluminum system	Elastic Modulus (GPa)		Error relative to the experimental results
	Current Simulation	Experimental data	
Single Crystal	64.14	63.55 [26]	0.93%
Nanocrystalline (grain diameter = 11.1 nm)	57.5 ± 0.32	60.2 [16]	4.45%

Furthermore, an analysis was performed to investigate the effect of various grain sizes on mechanical properties, similar to the work of Schiotz et al. [1]. A nanocrystalline aluminum structure with various mean grain diameters (4.29 to 13.82 nm) was simulated at a finite temperature (300K). The stress-strain curve is shown in Figure 3-4. It is observed that the plastic region is strongly dependent on the mean grain diameter, with the yield and ultimate strength increasing with increasing diameter i.e. the reverse Hall-Petch relation.

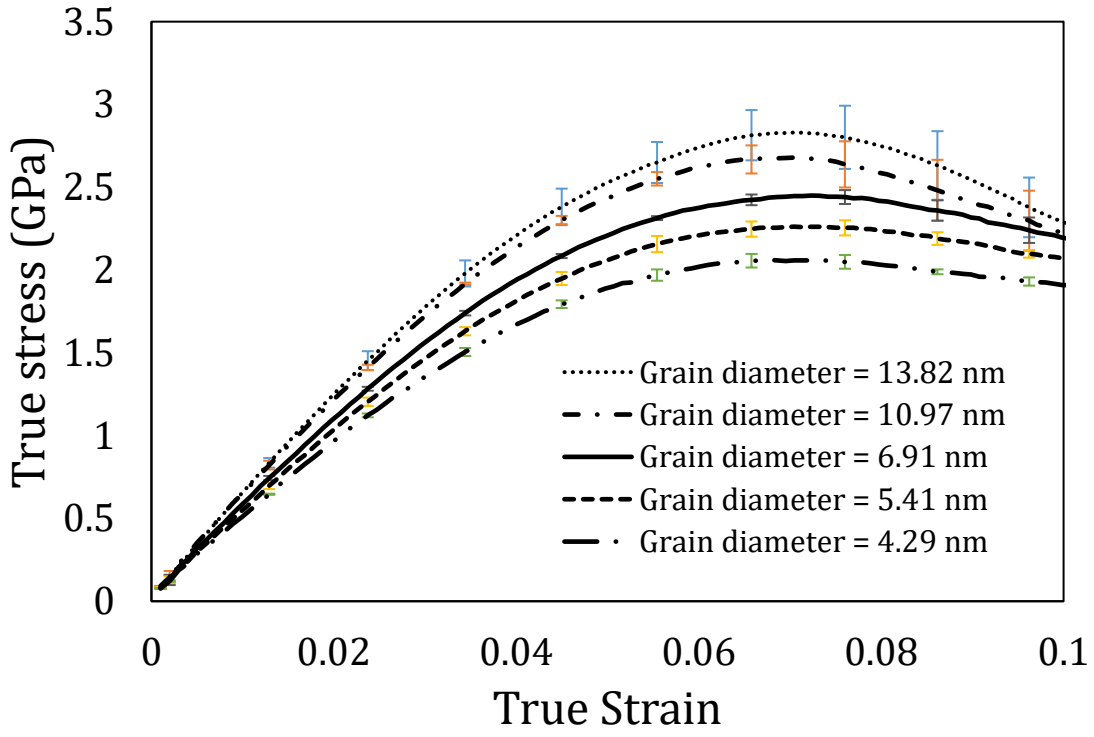

Figure 3-4: Stress-strain curves for nanocrystalline Aluminum with various grain numbers at 300K; the error bars indicate the uncertainty of the average (1σ).

From the stress-strain curves, the elastic moduli were determined within the linear region (ε = 2%). Elastic modulus ranged from 45.16 to 59.73 GPa at 300K. As well, it is evident that elastic modulus decreases with decreasing mean grain diameter as observed in previous research [1]. As the grain size decreases, there becomes a significantly higher portion of grain boundary atoms as compared to bulk FCC atoms. These grain boundary atoms have different structure and properties, which lead to a decrease in the overall elastic modulus [28].

Further, the yield stress is calculated using the 0.02% offset. The yield stresses are over-estimated compared to typical values of yield stress for macroscale aluminum, as shown in Figure 8. This result is typical of MD simulations due to the length scale limitations as the

proper sampling of defects such as vacancies, impurities, and dislocations cannot be investigated as what is observed in the macroscale structure [25]. In addition, Figure 3-5 and 3-6 show the reverse Hall-Petch relation for a nanocrystalline aluminum, i.e. a softening of the material as the grain size is reduced. These findings are supported by the work of Schiotz et al. [1] and Xu et al. [5] who also observed a reverse Hall-Petch relationship for nanocrystalline copper and aluminum, respectively. In addition to elastic modulus and yield stress, Poisson's ratio was also investigated for various grain sizes. From Figure 3-7, it is observed that the effect of grain sizes on Poisson's ratio was similar to the results in literature [8], in that the effect of grain size on Poisson's ratio is negligible.

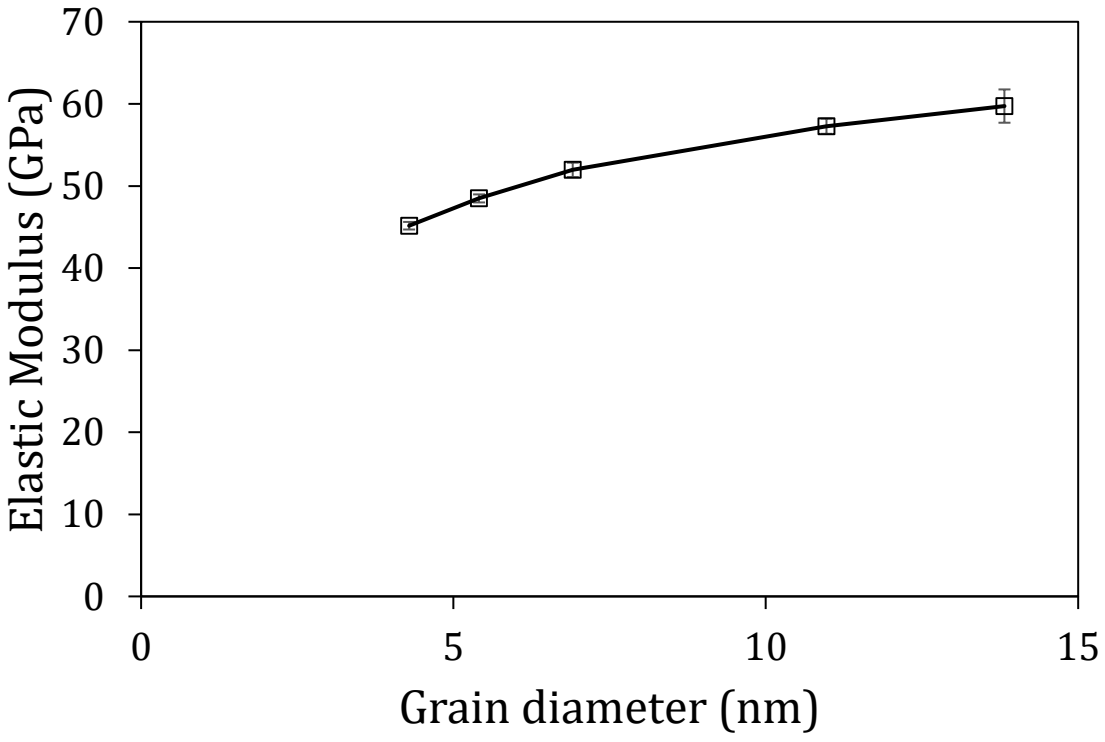

Figure 3-5: Elastic modulus for nanocrystalline Aluminum with various grain diameters at 300K.

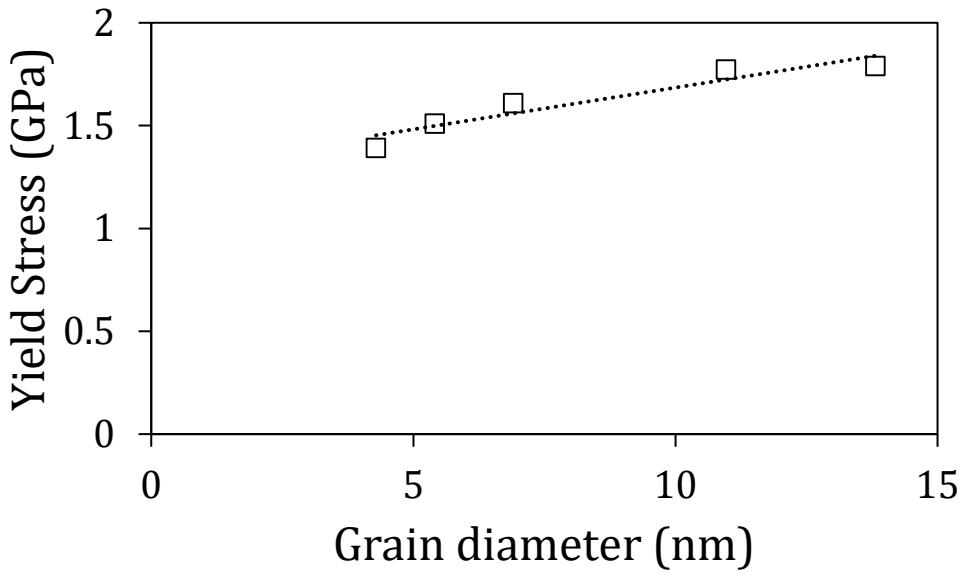

Figure 3-6: Estimation of yield stress for nanocrystalline Aluminum with different grain diameters at 300K.

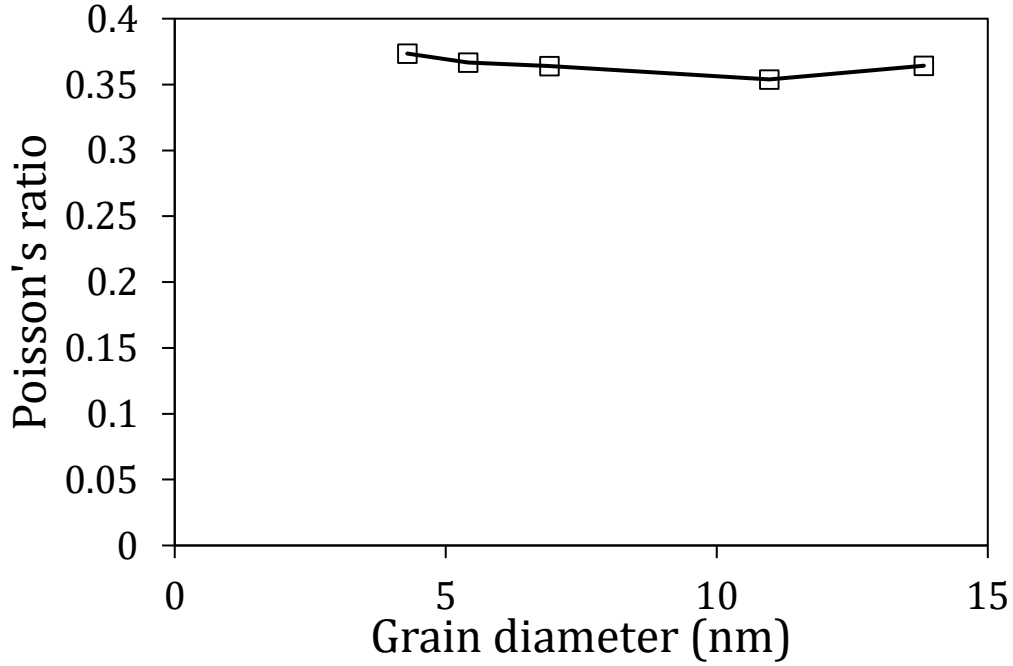

Figure 3-7: Poisson's ratio for nanocrystalline Aluminum with various grain diameters at 300K.

3.4.3. Effect of temperature on estimating mechanical properties

After investigating the effect of strain rate and grain size, the effect of various temperatures on the mechanical behavior of nanocrystalline aluminum with a constant mean grain diameter of 6.91nm was investigated. The stress-strain response over the 10% deformation for each temperature was determined, shown in Figure 3-8. It is observed that the mechanical properties decrease with increasing temperature. Hence, softening of the materials occurs due to increasing temperature. Due to the small system size, there exists small standard deviations in the stress-strain curve. This can be attributed to the nucleation of dislocations [1, 3].

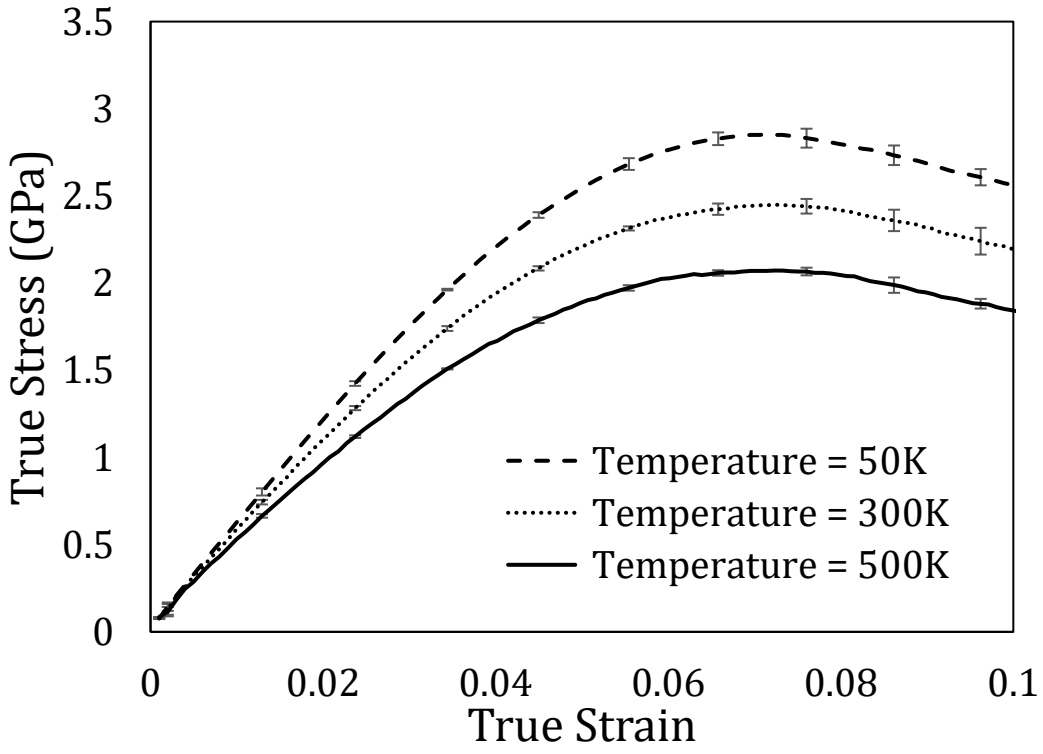

Figure 3-8: Effect of temperature on the stress-strain curve for a nanocrystalline aluminum with average grain boundary 6.91 nm; the error bars indicate the uncertainty of the average (1σ).

The elastic modulus and Poisson's ratio were obtained from the stress-strain curve for various mean grain sizes at different temperatures (50K-500K). From Figure 3-9, the curves follow a similar trend for the various temperatures. However, the value of elastic modulus decreases with increasing temperature, i.e. material softens as temperature increases. Also, the elastic modulus increases with increasing mean grain diameter. Hence, more grain boundaries leads to softer materials, which is the reverse Hall-Petch relation. As well, Poisson's ratio was estimated and shown in Figure 3-10. The effect of temperature on Poisson's ratio is minimal, similar to the findings in literature [7].

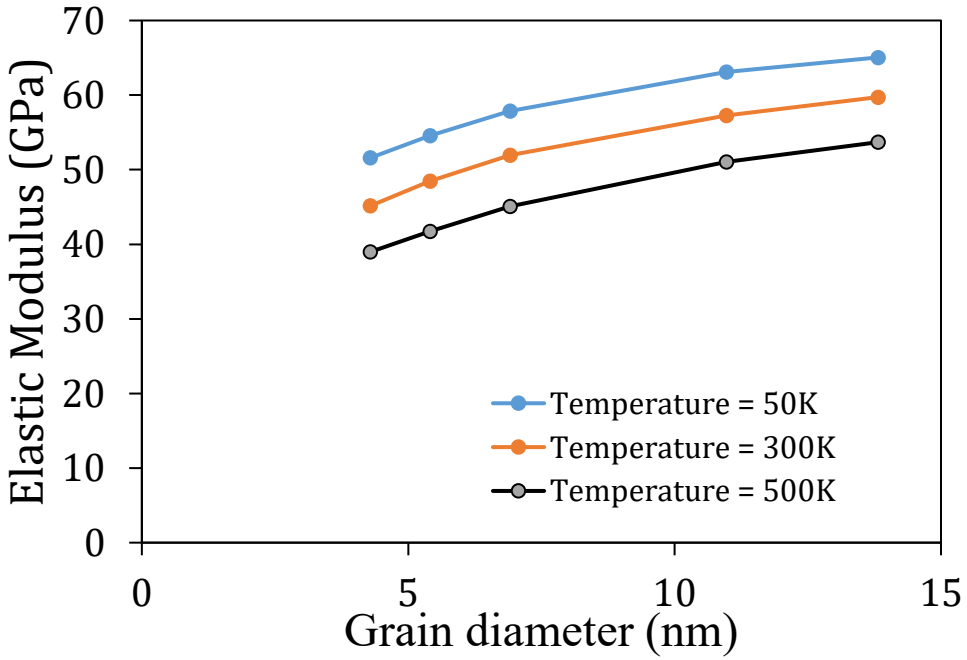

Figure 3-9: Effect of temperature on estimating elastic modulus for a nanocrystalline aluminum with various grain diameter.

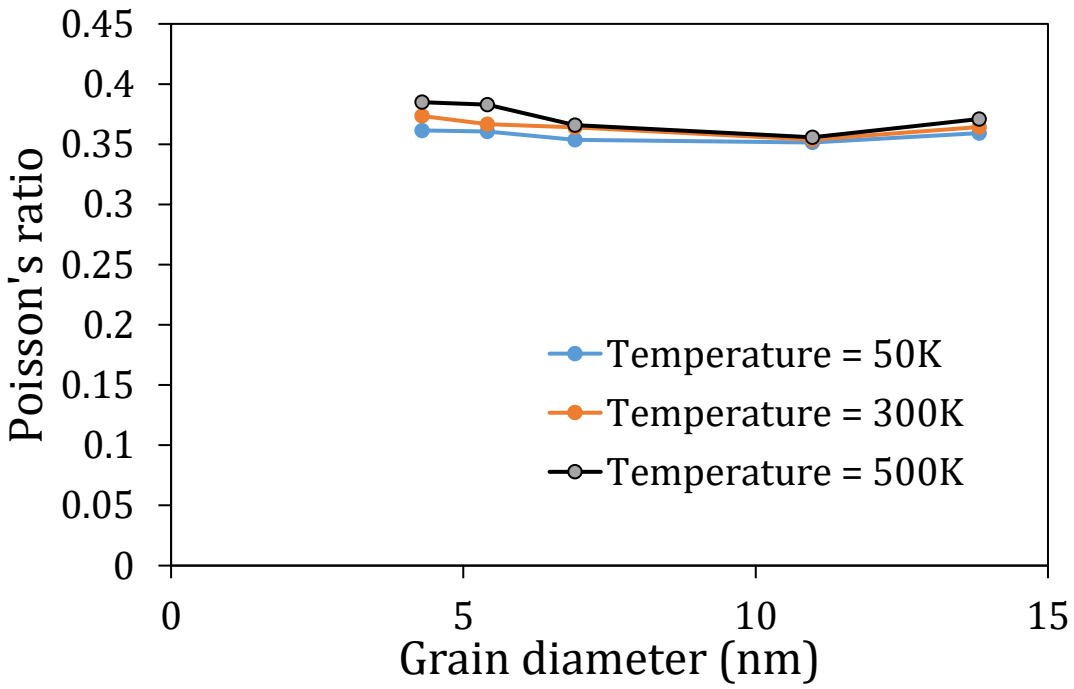

Figure 3-10: Effect of temperature on determining Poisson's ratio for a nanocrystalline aluminum with different grain diameter.

3.4.4. Crystal Structure

At the atomistic level, the crystal structure changes with the various grain size and strain for a nanocrystalline material. Figure 3-1 shows the change of the structure for initial case and after 10% strain for a grain diameter of 6.91 nm at 300K. Some new grain boundaries grow in the system, as highlighted in Figure 3-1, which is also the path for dislocation movement. Also, the nucleation of the atoms at the grain boundaries due to deformation is observed in the system. From Figure 3-11, the different structured atoms are compared as a function of strain for various temperatures. Initially, the system is almost entirely FCC structure, ranging from 80-90%; however, with continual strain, the atoms begin to rearrange into different structures, such as HCP. For the 6.91nm grain size, the percent FCC reduces by approximately 10%. As such, with increasing strain, the structure

changes from almost entirely FCC to a mixture of FCC and other structures indicating the increase of faults and dislocations within the system. It can also be seen that there is minimal effect of temperature to influence the development of these various different atom structures in the system throughout deformation.

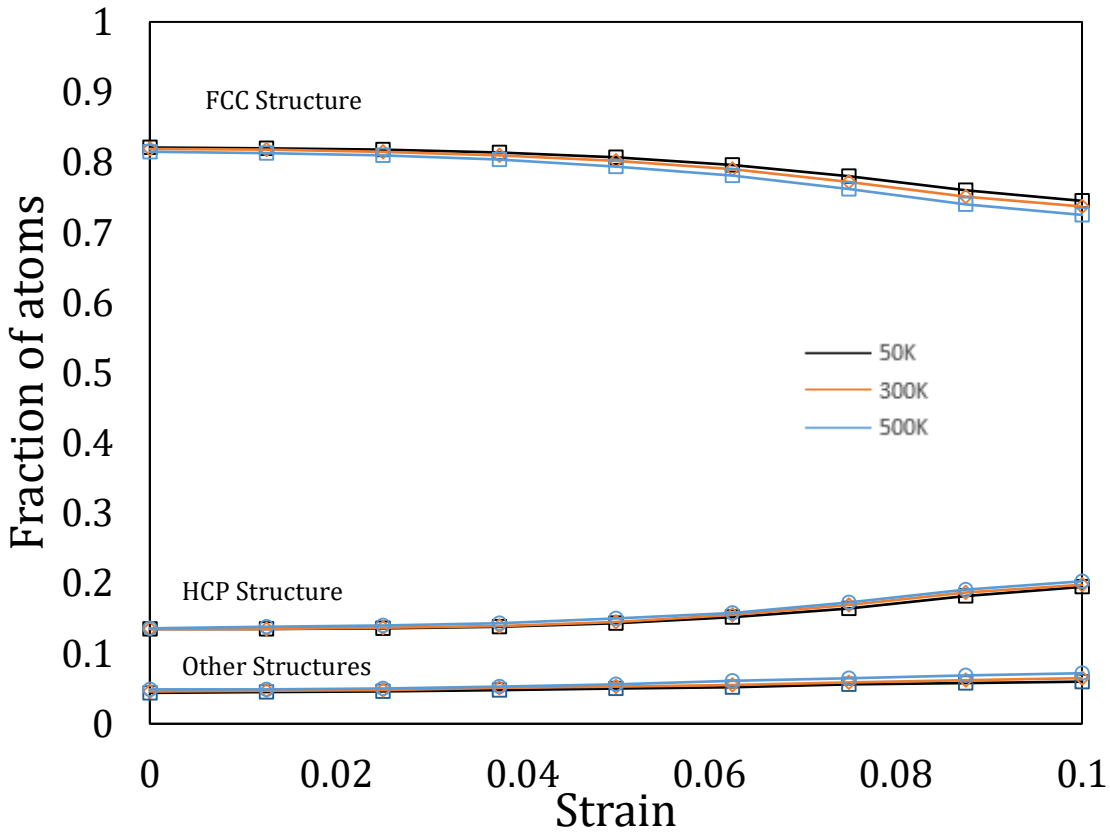

Figure 3-11: Structural changes as a function of the strain, for simulation at 50K, 300K and 500K for grain size 6.91 nm.

In Figure 3-12, the effect of various mean grain diameters on the crystal structure of the system is shown. Initially, the system contains around 80-90% FCC structured aluminum atoms, with the remaining being HCP or other structures. The HCP and other structured atoms are distributed to make grain boundaries in the system, whereas the FCC structured

atoms are atoms within the grains. Hence, the grain boundaries themselves are a type of fault in the system. As the mean grain diameter increased, the fraction of FCC atoms in the system increased whereas the fraction of HCP and other structured atoms decreased. This is expected since, as grains become bigger, more FCC atoms are required to fill each grain. As well, as grains become bigger there are less grain boundaries present in the simulation cell, hence the proportion of FCC structure atoms increases. After deforming the system by 10% strain at 300K, the FCC structure decreased by about 8.0% from the initial structure at all grain sizes. This decrease in FCC structure leads to an increase in HCP and Other structures by about 6.2% and 1.8%, respectively. From Figures 3-11 and 3-12, it is clear that the HCP atoms (stacking faults) increased due to the movement of dislocations throughout the grains. As well, it is clear that Other structured atoms increased due to the increase of atoms near grain boundaries during deformation. These effects on HCP and Other structured atoms are shown in Figure 3-13.

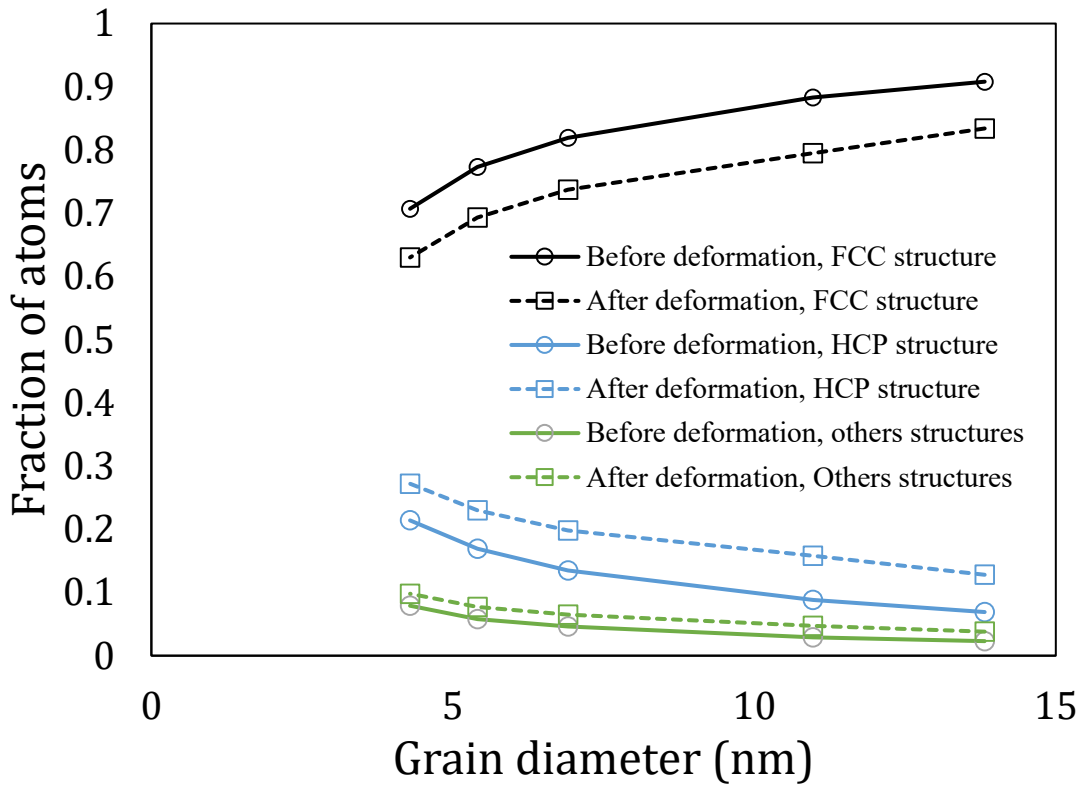

Figure 3-12: Comparison of the fraction of atoms in a given local crystal structure as a function of the grain diameter for initial condition before deformation (open circle) and after deformation (open square) by 10% for simulation at 300K.

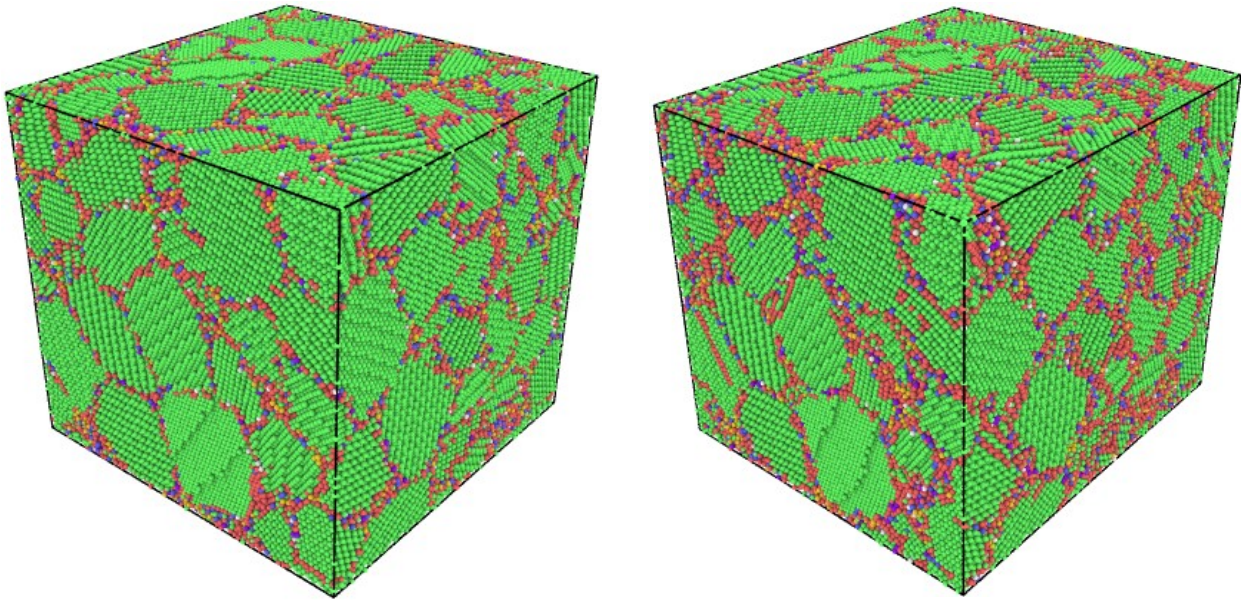

(a) (b)

Figure 3-13: System (a) at initial, and (b) after deformation showing the change of structure with the increment of HCP and other structured atoms as decrease in FCC atoms. Green colored atoms are in perfect FCC structure, Red atoms are in HCP structure and Blue atoms are Other structures atoms structure.

3.5. Conclusions

Researchers in the field of material science are utilizing MD simulations more frequently to study the mechanical behaviors of materials. In the present study, a uniaxial tensile test using MD simulation was performed to estimate the mechanical properties of a nanocrystalline aluminum with various nano-sized grains (4.29 to 13.82 nm). Mechanical properties such as elastic modulus, Poisson's ratio, and yield stress were determined.

For various mean grain diameters, the elastic modulus ranged from 45.16 to 59.73 GPa at 300K. It is observed that the atoms fraction for the grain boundary atoms as compared to bulk FCC atoms increases with decreasing grain size. These grain boundary atoms have different structures and properties than atoms within grains, leading to a decrease in the overall elastic modulus. Due to the length scale limitations of MD simulations, the yield stresses were over-estimated in the present study, similar to other MD works. Both elastic modulus and yield stress increased with increasing grain diameter, which followed the reverse Hall-Petch relationship of the material. In addition, the Poisson's ratio predicted showed minimal deviation from the experimental data due to changes in mean grain diameter.

Next, the effect of strain rate and temperature on estimating mechanical properties was investigated. Results showed the mechanical properties are independent of strain rates used in the present study. Various temperatures were studied to analyze the behavior of the system. It was shown that the systems became softer with increasing temperature. Since the system was in atomistic-scale, small standard deviations of the stress at higher values of strain were observed. In addition, the change in the crystal structure due to the deformation in the various grain sizes was investigated to conclude the effect of crystal orientation on the mechanical behavior of nanocrystalline materials. Results showed that the FCC structure decrease by around 8.0% compared to the initial structure, which indicates a growth in HCP atoms and other structures by approximately 6.2% and 1.8%, respectively.

References

1. Schiøtz, J., Vegge, T., Di Tolla, F. D., and Jacobsen, K. W. (1999). Atomic-scale simulations of the mechanical deformation of nanocrystalline metals. *Physical Review B*, *60*(17), 11971.
2. Suryanarayana, C. (1995). Nanocrystalline materials. *International Materials Reviews*, *40*(2), 41-64.
3. Jacobsen, K. W., Stoltze, P., and Nørskov, J. K. (1996). A semi-empirical effective medium theory for metals and alloys. *Surface Science*, *366*(2), 394-402.
4. Schiøtz, J., Di Tolla, F. D., and Jacobsen, K. W. (1998). Softening of nanocrystalline metals at very small grain sizes. *Nature*, *391*(6667), 561.
5. Xu, W., and Dávila, L. P. (2018). Tensile nanomechanics and the Hall-Petch effect in nanocrystalline aluminium. *Materials Science and Engineering: A*, *710*, 413-418.
6. Mishin, Y., Farkas, D., Mehl, M. J., and Papaconstantopoulos, D. A. (1999). Interatomic potentials for monoatomic metals from experimental data and ab initio calculations. *Physical Review B*, *59*(5), 3393.
7. Kadau, K., Lomdahl, P. S., Holian, B. L., Germann, T. C., Kadau, D., Entel, P., and Westerhoff, F. (2004). Molecular-dynamics study of mechanical deformation in nano-crystalline aluminum. *Metallurgical and materials transactions A*, *35*(9), 2719-2723.
8. Galanis, N. V., Remediakis, I. N., and Kopidakis, G. (2010). Mechanical response of nanocrystalline Cu from atomistic simulations. *physica status solidi c*, *7*(5), 1372-1375.

9. Kraus, Z. (2014). *Computational tools for preliminary material design of metals and polymer-ceramic nano composites* (Doctoral dissertation, Georgia Institute of Technology).
10. Hirel, P. (2015). Atomsk: a tool for manipulating and converting atomic data files. *Computer Physics Communications*, *197*, 212-219.
11. Okabe, A., Boots, B., Sugihara, K., and Chiu, S. N. (2009). *Spatial tessellations: concepts and applications of Voronoi diagrams* (Vol. 501). John Wiley and Sons.
12. Chen, D. (1995). Structural modeling of nanocrystalline materials. *Computational materials science*, *3*(3), 327-333.
13. Van Swygenhoven, H., and Caro, A. (1997). Plastic behavior of nanophase Ni: A molecular dynamics computer simulation. *Applied Physics Letters*, *71*(12), 1652-1654.
14. Van Swygenhoven, H., and Caro, A. (1997). Molecular dynamics computer simulation of nanophase Ni: structure and mechanical properties. *Nanostructured materials*, *9*(1-8), 669-672
15. Kumar, S., Kurtz, S. K., Banavar, J. R., and Sharma, M. G. (1992). Properties of a three-dimensional Poisson-Voronoi tesselation: A Monte Carlo study. *Journal of statistical physics*, *67*(3-4), 523-551.
16. Haque, M. A., and Saif, M. A. (2002). Mechanical behavior of 30–50 nm thick aluminum films under uniaxial tension. *Scripta Materialia*, *47*(12), 863-867.
17. Becker, C. A., Tavazza, F., Trautt, Z. T., and de Macedo, R. A. B. (2013). Considerations for choosing and using force fields and interatomic potentials in materials science and engineering. *Current Opinion in Solid State and Materials Science*, *17*(6), 277-283.

18. Hale, L. M., Trautt, Z. T., and Becker, C. A. (2018). Evaluating variability with atomistic simulations: the effect of potential and calculation methodology on the modeling of lattice and elastic constants. *Modelling and Simulation in Materials Science and Engineering*, *26*(5), 055003.
19. Plimpton, S. (1995). Fast parallel algorithms for short-range molecular dynamics. *Journal of computational physics*, *117*(1), 1-19.
20. Thompson, A. P., Plimpton, S. J., and Mattson, W. (2009). General formulation of pressure and stress tensor for arbitrary many-body interaction potentials under periodic boundary conditions. *The Journal of chemical physics*, *131*(15), 154107.
21. Morrissey, L. S., Handrigan, S. M., Subedi, S., and Nakhla, S. (2019). Atomistic uniaxial tension tests: investigating various many-body potentials for their ability to produce accurate stress strain curves using molecular dynamics simulations. *Molecular Simulation*, *45*(6), 501-508.
22. S. A. Etesami, M. Laradji and E. Asadi, "Interatomic potentials transferability in predicting temperature dependency of elastic constants for titanium, zirconium and magnesium," *Modell Simul Mater Sci Eng,* 2018.
23. Lysogorskiy, Y. V., Hammerschmidt, T., Janssen, J., Neugebauer, J., and Drautz, R. (2019). Transferability of interatomic potentials for molybdenum and silicon. *Modelling and Simulation in Materials Science and Engineering*.
24. Subedi, S., Morrissey, L. S., Handrigan, S. M., and Nakhla, S. The effect of many-body potential type and parameterization on the accuracy of predicting mechanical properties of aluminum using molecular dynamics. *Molecular simulation* (Accepted)

25. Handrigan, S. M., Morrissey, L. S., and Nakhla, S. (2019). Investigating various many-body force fields for their ability to predict reduction in elastic modulus due to vacancies using molecular dynamics simulations. *Molecular Simulation*, 1-12.
26. Vallin, J., Mongy, M., Salama, K., and Beckman, O. (1964). Elastic constants of aluminum. *Journal of Applied Physics*, *35*(6), 1825-1826.
27. Subramaniyan, A. K., and Sun, C. T. (2008). Continuum interpretation of virial stress in molecular simulations. *International Journal of Solids and Structures*, *45*(14-15), 4340-4346.
28. Chaim, R., and Hefetz, M. (2004). Effect of grain size on elastic modulus and hardness of nanocrystalline ZrO 2-3 wt % Y 2 O 3 ceramic. *Journal of materials science*, *39*(9), 3057-3061.

4. Chapter 4: Conclusion and Future work

4.1.Conclusion:

In recent years, MD is becoming a reliable tool to engineers and scientists to understand the chemical and mechanical behavior of materials. This thesis focuses on the study of mechanical deformation of single crystal and nanocrystalline aluminum. In addition, the various many-body interatomic potentials were tested for their accuracy in predicting mechanical property for the single crystal aluminum. Elastic modulus and Poisson's ratio were calculated and compared with available experimental data.

In Chapter 2, the author has used fourteen various interatomic potentials to simulate uniaxial tension tests at the atomistic level at room temperature. It was shown that the various parameterizations of the potentials profoundly influenced the prediction of elastic modulus and Poisson's ratio. The interatomic potentials that were parameterized with elastic constants at room temperature were the most accurate. Whereas the other potentials either under or over predicted the results. Out of the fourteen available potentials, the Mishin et al. EAM potential showed the highest accuracy with an error less than 1%.

In Chapter 3, the author has used the most accurate potential from Chapter 2 to simulate uniaxial tension in MD for nanocrystalline aluminum with various grain sizes (4.29 to 13.82 nm). The results were compared with available experimental data to validate the simulation. It was shown that as grain size decreased, the proportion of atoms within grain boundaries increased compared to bulk FCC atoms. The atoms within grain boundaries have different structures and properties, thus a decrease in the elastic modulus with decrease in grain size was observed. As such, the reverse Hall-Petch relationship was investigated.

Furthermore, the effect of strain rate and temperature on nanocrystalline aluminum was investigated. It was shown that the FCC structure decreased by approximately 8.0% compared to the initial structure, which indicated a growth in HCP atoms and other structures by approximately 6.2% and 1.8%, respectively.

4.2. Future Work:

The author proposed different future works, which are listed below.

- Investigation of mechanical properties for aluminum alloys.
- Effect of porosity and defects on estimating mechanical properties of aluminum.
- Study of the change in the structural and mechanical behavior of aluminum due to corrosion.

Appendix A:

Validation of Numerical Procedure

Prior to studying nanocrystalline aluminum, the numerical simulation procedure was validated with available literature [1] for a nanocrystalline copper with a mean grain diameter of 5.21 nm at 300K. The following steps were performed to validate the numerical procedure

- Nanocrystalline copper was created utilizing atomsk [2] with mean grain diameter 5.21 nm.
- Then, the sample was deformed under uniaxial loading in MD simulation using EMT potential utilizing LAMMPS.
- Results from five randomly oriented nanocrystalline copper were averaged to obtain the stress-strain curve as shown in Figure A.

From Figure A, it was observed that the numerical procedure utilized in the current study successfully captured the trend from literature. As such, the authors are confident in applying the numerical procedure to various nanocrystalline materials.

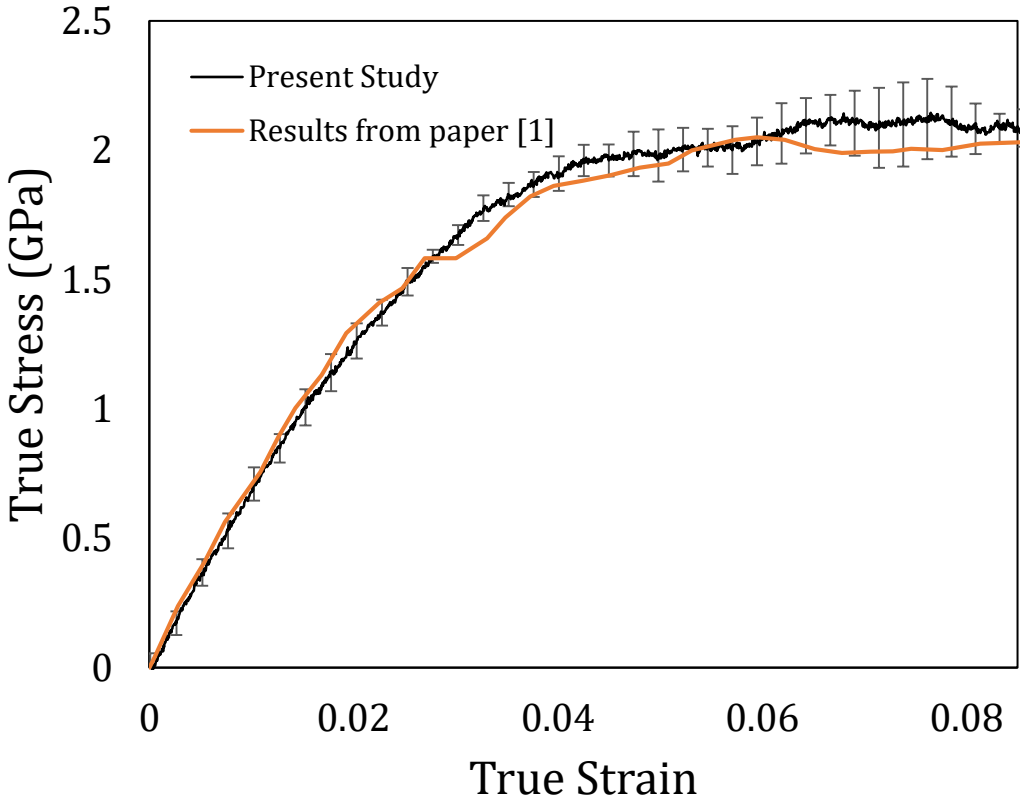

Figure A: Validation of the Simulation method with the published research [1] for nanocrystalline Copper for an average grain diameter of 5.21 nm at 300K. The stress-strain curve at strain rate of 5×10^8 s^{-1} for an average of five simulations with 100,000 atoms compared with literature [1].

Reference:

1. Schiøtz, J., Vegge, T., Di Tolla, F. D., and Jacobsen, K. W. (1999). Atomic-scale simulations of the mechanical deformation of nanocrystalline metals. *Physical Review B*, *60*(17), 11971.
2. Hirel, P. (2015). Atomsk: a tool for manipulating and converting atomic data files. *Computer Physics Communications*, *197*, 212-219.